



**Northwest and  
Alaska Fisheries  
Center**

National Marine  
Fisheries Service

U.S. DEPARTMENT OF COMMERCE

**NWAFRC PROCESSED REPORT 84-20**

Physical Factors  
Affecting the Fate  
of a Petroleum Spill  
in the  
Southeastern Bering Sea

December 1984

## **NOTICE**

This document is being made available in .PDF format for the convenience of users; however, the accuracy and correctness of the document can only be certified as was presented in the original hard copy format.

Inaccuracies in the OCR scanning process may influence text searches of the .PDF file. Light or faded ink in the original document may also affect the quality of the scanned document.



PHYSICAL FACTORS AFFECTING THE  
FATE OF A PETROLEUM SPILL IN THE  
SOUTHEASTERN BERING SEA

By

Robert K. Miyahara

and

W. James Ingraham, Jr.

National Oceanic and Atmospheric Administration  
National Marine Fisheries Service  
Northwest and Alaska Fisheries Center  
Resource Ecology and Fisheries Management Division  
Resource Ecology and Ecosystem Simulation Task  
7600 Sand Point Way N.E.  
Building 4, BIN C15700  
Seattle, Washington 98115

December 1984

## CONTENTS

	Page
Tables and Figures . . . . .	i
Introduction. . . . .	1
Climate and Weather . . . . .	3
Bathymetry . . . . .	12
Geological Oceanography	
Sediments . . . . .	14
Suspended Particulate Matter . . . . .	18
Physical Oceanography	
River Runoff . . . . .	28
Tides . . . . .	30
Non-Tidal Currents . . . . .	35
Water Temperatures . . . . .	38
Ice . . . . .	46
Salinities . . . . .	48
Vertical Water Structure and Seasonal Changes . . . . .	51
Chemical Oceanography	
Nutrient Salts . . . . .	53
Dissolved Hydrocarbons . . . . .	57
References . . . . .	62

Table 1.--Annual average weather data.

Table 2.--Monthly weather conditions for King Salmon and Bethel, Alaska  
(Brower et al., 1977 and Ruffner et al., 1978).

Table 3.--Average (a) surface and (b) near-bottom concentrations (nl/l, STP)  
of methane, ethane, ethene, propane, and propene for various water  
depth intervals (Cline, 1981).

Figure 1.--Monthly mean insolation (KJ/M<sup>2</sup>·Day) for each month (Durrenberger,  
R.W., 1980).

Figure 2.--Monthly mean cloud cover for King Salmon and Bethel, Alaska  
(Ruffner, 1978).

Figure 3.--Vector mean wind speeds (m/sec) and directions for each month  
(Brower et al., 1977).

Figure 4.--Long term mean (LTM) sea level pressure -1000(mb) fields by month.

Figure 5.--Bathymetry (m) of the southern Bering Sea shelf.

Figure 6.--Sediment mean size distribution (Sharma, 1979).

Figure 7.--Grain size sorting (Sharma, 1979).

Figure 8.--Weight percent in sediment (a) Silt, (b) Clay (Sharma, 1979).

Figure 9.--Weight percent organic carbon in sediment (Sharma, 1979).

Figure 10.--Water depth (m) versus sediment size ( $\phi$ ) for the Bering Shelf  
(Sharma, 1979)

Figure 11a.--Satellite imagery showing relative suspended load in near-  
surface waters on October 15, 1973 (Sharma, 1979).

Figure 11b.--Satellite imagery showing relative suspended load in near-  
surface waters on November 5, 1983 (Sharma, 1979).

- Figure 12.--Distribution of total suspended matter (a) at the surface and (b) 5 meters above the bottom in the southeastern Bering Shelf (cruise RP-4-D: 75-B-III, 12 September - 5 October 1975 (Feely et al., 1981)).
- Figure 13.--Net particulate attenuation profiles, stability profiles, and density profiles from the (a) coastal, (b) middle, and (c) outer-shelf domains (Baker, 1983).
- Figure 14a.--Attenuation (top) and density (bottom) cross-sections for line 2 (station NA 34-40), August 1980 (Baker, 1983).
- Figure 14b.--Attenuation (top) and density (bottom) cross-sections for line 2 (station NA 34-40), January 1981 (Baker, 1983).
- Figure 14c.--Attenuation (top) and density (bottom) cross-sections for line 2 (station NA 34-40), May 1981 (Baker, 1983).
- Figure 15.--Average monthly precipitation and riverine runoff for the Kuskokwim River (Data from Ruffner et al., 1978 and Roden, 1967).
- Figure 16a.--Co-tidal chart of the semi-diurnal component  $M_2$ . Dots refer to the stations (Pearson et al., 1981).
- Figure 16b.--Co-tidal chart of the semi-diurnal component  $N_2$  (Pearson et al., 1981).
- Figure 16c.--Co-tidal chart of the diurnal component  $K_1$  (Pearson et al., 1981).
- Figure 16d.--Co-tidal chart of the diurnal component  $O_1$  (Pearson et al., 1981).
- Figure 17a.-- $M_2$  current ellipses (Pearson et al., 1981).
- Figure 17b.-- $K_1$  current ellipses (Pearson et al., 1981).
- Figure 18.-- Mean circulation of southeastern Bering Sea (Kinder and Schumacher, 1981).
- Figure 19a.--Average surface temperatures ( $^{\circ}\text{C}$ ) months 1 to 6.
- Figure 19b.--Average surface temperatures ( $^{\circ}\text{C}$ ) months 7 to 12.

Figure 20a.--Average bottom temperatures ( $^{\circ}\text{C}$ ) months 1 to 6.

Figure 20b.--Average bottom temperatures ( $^{\circ}\text{C}$ ) months 7 to 12.

Figure 21.-- DYNUMES area 1 to 3.

Figure 22.--Surface temperature anomalies - DYNUMES areas 1 to 3 (Pola Swan and  
Ingraham, 1984).

Figure 23.--Bottom temperature anomalies - DYNUMES area 1 to 3 (Pola Swan and  
Ingraham, 1984).

Figure 24.--Approximate ice edge of each month (Brower et al., 1977)

Figure 25.--Long-term mean sea surface salinity ( $^{\circ}/\text{oo}$ ) for January to March,  
May, July, and September (Ingraham, 1981).

Figure 26.--Long-term mean bottom salinity ( $^{\circ}/\text{oo}$ ) for January to March, May,  
July, and September (Ingraham, 1981).

Figure 27.--Locations of the domains (coastal, middle, and oceanic) and fronts  
(inner, middle, and shelf break) over the eastern Bering Sea shelf  
(Kinder and Schumacher, 1981).

Figure 28.--Temperature-salinity and nutrient-salinity envelopes in the eastern  
Bering Sea in July 1978 (Hattori and Goering, 1981).

Figure 29.--Ammonium ( $\text{mg at N/l}$ ) cross section in outer Bristol Bay south of  
Pribolif Islands during 29-31 May 1979 (Hattori and Goering, 1981).

Figure 30.--(a) Surface and (b) near-bottom distributions of dissolved methane  
during July 1976 (Cline, 1981).

Figure 31.--Surface distribution of dissolved ethene ( $\text{nl/l, STP}$ ) in July 1976  
(Cline, 1981).

## Introduction

In examining the potential environmental impact of oil development on marine ecosystems of the southeastern Bering Sea, two important factors which determine the distribution, weathering, persistence and toxicity of inadvertently induced oil are (1) the physical/chemical properties of oil itself, and (2) the physical characteristics of this particular regional environment. Because of the great number of possible combinations of elements within these factors, no two oil contamination events are the same in behavior and environmental impact. Properties differ from various crude oils and their distilled products. Also, crude oil properties vary from region to region, well to well, and even according to the depth of a well. The physical factors of the local environment include the regional climatology, meteorology, oceanography, hydrology, and geology. These are discussed here to illustrate the background information available about these primary agents which play a major roll in determining the ultimate fate of any oil induced into this ecosystem.

This summary information is compiled for three primary areas-- offshore of Port Moller, Port Heiden, and Cape Newenham. Its inherent nature includes diurnal, monthly, seasonal, annual, and inter-annual variations. Therefore, annual, seasonal, and monthly data averages are presented where possible as well as extreme conditions. Much of the data, however, does not exist or is unavailable for all seasons. In some cases most of the data were taken only during the summer months, permitting no description of seasonal change. A purposeful attempt was made to present the information in self-explanatory form

in the following tables, illustrations, and graphs. This material will hopefully serve as background for evaluation of the effects of oil development and as background information for possible future monitoring of changes.

### Climate and Weather

Consideration of the seasonal climatology of the eastern Bering Sea gives us expected values and extremes for the major physical phenomenon and external forces which affect spilled petroleum from above--sunlight, air temperature, precipitation, and wind.

Sunlight measured at King Salmon and Bethel in terms of insolation (Incident Solar Radiation) with both direct and diffuse radiation, varies considerably from the winter minimum ( $<1 \text{ KJ/M}^2$ ) in December to the summer maximum ( $17 \text{ KJ/M}^2$ ) in June (Figure 1). Although the annual change is large due to the high northerly latitude, the monthly change is smooth. The slight asymmetry in the curve may be explained by examining the monthly mean cloud cover (Figure 2). Somewhat contrary to what might be expected, the stormy winter months average the clearest sky with minimum cloud cover from January to March. Maximum cloud cover occurs in summer from July to August. Thus, the solar insolation which reaches the surface is slightly lower during the more cloudy cooling period from June to December than during the corresponding month of the less cloudy warming period from December to June. As expected, a large monthly change in air temperatures follows the large monthly changes in insolation.

About a half century of weather records (air temperature, precipitation, and wind) from coastal reporting stations were summarized by Brower et. al. (1977). Although the four stations in the Bristol Bay area show very similar data patterns, slight differences are apparent in the overall annual averages of weather data (Table 1). Cape Newenham and King Salmon farther north, have more northerly winds from the land, and are about one degree colder than Port Moller and Port Heiden on the south side of Bristol Bay. Southerly winds off the ocean at speeds of about  $5.1 \text{ m/sec}$  dominate at the southern

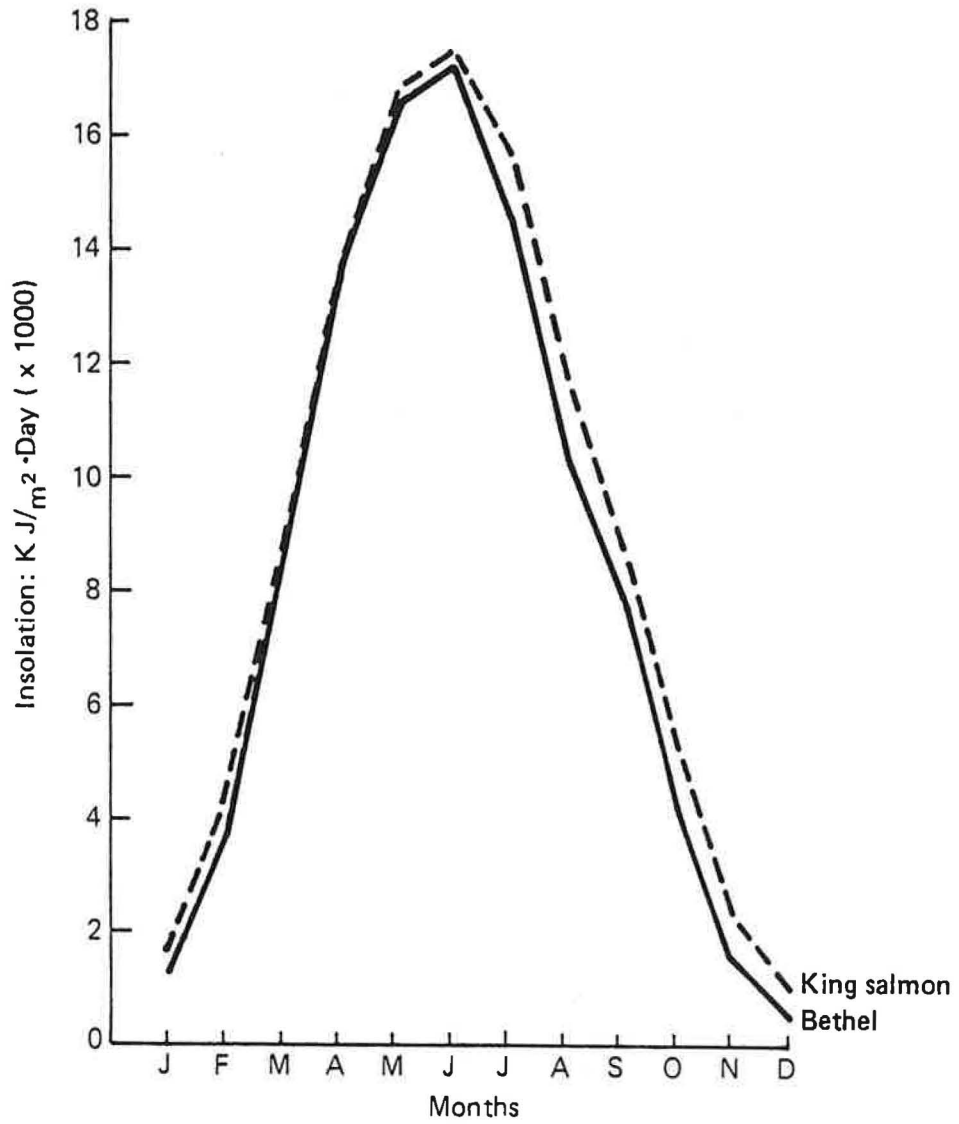


Figure 1.--Monthly mean insolation (KJ/M<sup>2</sup>·Day) for each month (Durrenberger, R.W., 1980).

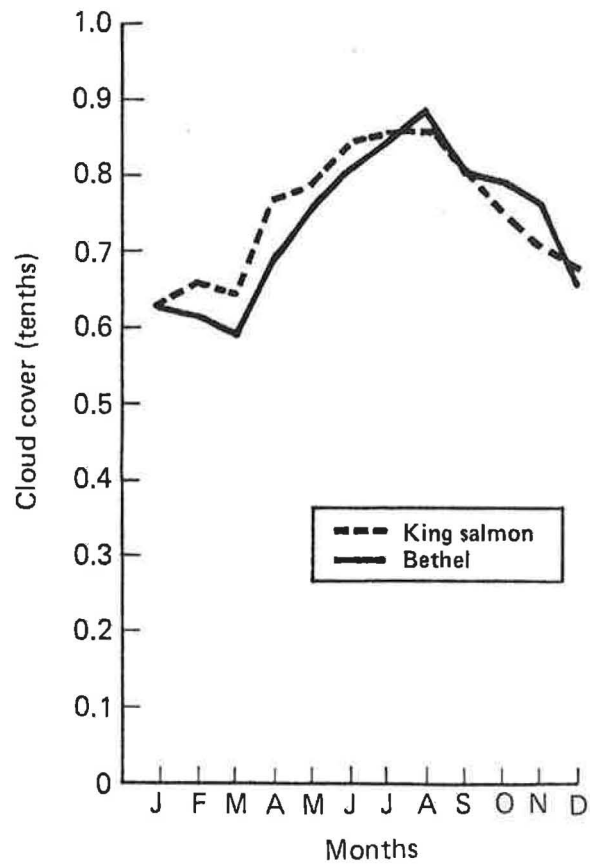


Figure 2.--Monthly mean cloud cover for King Salmon and Bethel, Alaska (Ruffner,1978).

Table 1.--Annual average weather data.

	Cape Newenham	King Salmon	Port Moller	Port Heiden
Maximum temperature (°C)	2.8	5.0	5.5	5.5
Average temperature (°C)	0.6	0.7	1.3	1.9
Minimum temperature (°C)	-1.7	-3.7	-2.9	-1.7
Total precipitation (cm)	94.6	50.2	110.5	37.2
Snowfall (cm)	206.2	113.3	233.9	158.2
Wind direction	N	N	S	ESE
Wind speed (m/sec)	5.0	4.7	4.5	6.6

stations suggesting a net annual air convergence over Bristol Bay. The seasonal data must be examined to see how this convergence relates to the precipitation maximum which occurs at the two westernmost stations.

The seasonal changes of weather from month to month can be clearly seen in the mean data from King Salmon (Table 2). Monthly mean data from Bethel which is just north of Bristol Bay is included for comparison to show the general similarity in station data along the southwestern Alaskan coast. The mean air temperatures are cyclic during the year from about  $-11^{\circ}$  to  $12^{\circ}\text{C}$ , alternating between below freezing then above freezing about six months at a time. This appears related to two distinct wind seasons, cold, relatively dry northerly (from the north) winds off the land from October to April, and warm, moist southerly winds off the ocean from May to September. Wind speeds average about 4.6 m/sec most of the year, then are slightly higher to 5.1 m/sec from February to May. Precipitation is low and consistent (about 25 mm) from December to May then increases about three fold during the peak in August.

More details about the consistency of the wind between stations may be derived from monthly vector averages (Figure 3). Vector mean speeds range from 0.4 to 2.4 m/sec, noticeably lower than the scalar averages of 4.6 to 5.1 m/sec discussed above. Mean wind vectors are lined up in the same direction at all stations only in the peak of winter and summer, from the northeast in December and from the southwest in July-August. In other months wind directions may vary between stations with the northern stations maintaining their northerly or easterly components well into the transition periods, and similarly the southern stations maintaining their southerly or westerly components. Therefore, the apparent convergence suggested in the annual averages is only developed during the transition periods between summer and winter.

King Salmon Lat: 58°41'N Long: 156°39'W

	Jan.	Feb.	Mar.	Apr.	May	Jun.	Jul.	Aug.	Sep.	Oct.	Nov.	Dec.	Ave.
Average Temp. [°C]													
Monthly	-10.3	-8.6	-6.4	-0.3	5.9	10.4	12.5	12.1	8.5	0.9	-5.5	-11.3	0.7
Daily Max.	-6.1	-4.1	-1.9	3.9	10.7	15.4	16.9	16.1	12.7	4.9	-1.7	-6.9	5.0
Daily Min.	-14.6	-13.0	-11.1	-4.6	1.0	5.4	8.0	8.2	4.3	-3.2	-9.4	-15.7	-3.7
Record High	8.3	7.8	12.2	15.6	23.9	26.7	29.4	28.9	23.3	16.7	8.9	8.9	
Record Low	-36.7	-40.6	-41.1	-20.0	-10.6	-1.7	0.6	0.0	-7.8	-18.3	-25.6	-34.4	
Wind													
Direction	N	N	N	NNW	S	SW	S	S	S	N	N	N	N
Speed [m/sec]	4.7	5.1	5.3	5.1	5.1	4.9	4.6	4.6	4.8	4.7	4.9	4.7	4.9
Precipitation [mm]													
Normal	23.9	25.1	29.5	22.9	28.7	36.6	55.4	87.9	78.0	50.8	36.3	26.7	501.7
Monthly Max.	76.7	76.2	61.2	75.9	61.0	96.0	100.0	163.6	185.4	161.3	75.2	86.9	
Monthly Min.	4.1	2.8	1.0	t	2.8	0.0	8.1	49.5	25.4	5.1	t	3.0	

Bethel Lat: 60°47'N Long: 161°48'W

Average Temp. [°C]													
Monthly	-14.9	-13.2	-11.4	-4.2	4.5	10.9	12.6	11.3	7.2	-1.0	-8.2	-15.3	-1.8
Daily Max.	-10.9	-9.0	-6.5	0.4	9.2	15.7	16.6	14.7	11.0	2.3	-4.7	-11.5	2.3
Daily Min.	-19.0	-17.5	-16.4	-8.7	-0.2	6.1	8.6	7.8	3.4	-4.3	-11.8	-19.2	-5.9
Record High	8.9	7.8	7.8	11.7	26.1	30.0	28.3	27.8	21.1	13.3	7.2	7.2	
Record Low	-43.3	-37.8	-39.4	-30.0	-15.6	-2.2	-0.6	0.6	-7.8	-20.6	-30.0	-37.2	
Wind													
Direction	NE	NNE	NNE	NW	S	NW	SSW	SSW	SSW	NNE	NE	NNE	NNE
Speed [m/sec]	6.2	6.6	6.0	6.0	5.3	5.1	5.1	5.1	5.0	5.6	6.0	6.2	5.7
Precipitation [mm]													
Normal	13.7	18.8	20.1	10.9	21.1	31.5	50.3	100.8	61.5	33.5	24.4	15.7	402.3
Monthly Max.	59.7	53.8	39.6	39.1	42.2	84.3	97.5	147.6	90.9	63.8	63.3	65.5	
Monthly Min.	1.5	0.8	0.5	1.5	2.5	6.4	16.8	43.4	10.7	2.8	1.0	2.8	

Table 2.--Monthly weather conditions for King Salmon and Bethel, Alaska  
(Brower et. al. 1977 and Ruffner et al. 1978)

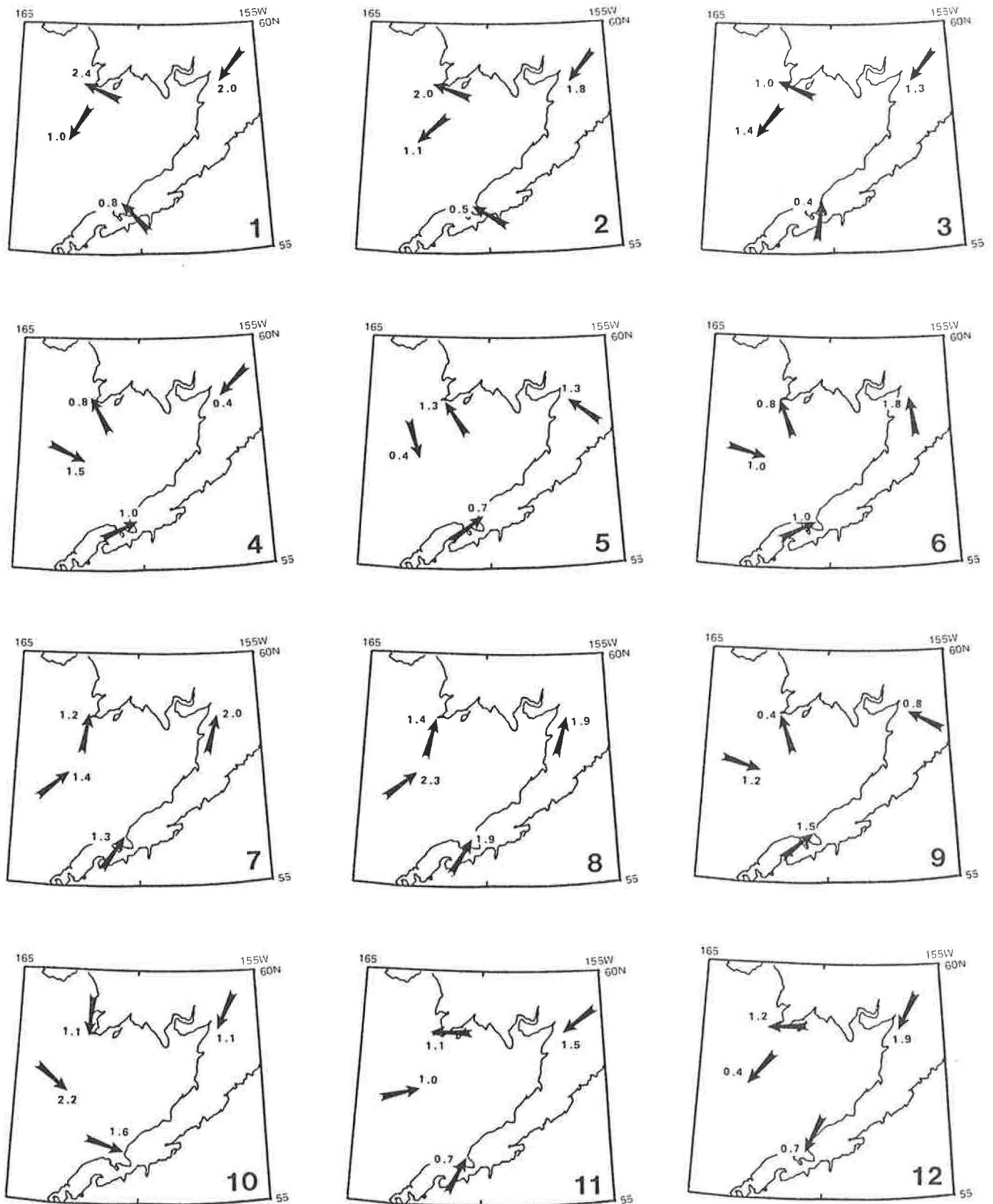


Figure 3.--Vector mean wind speeds (m/sec) and directions for each month (Brower et. al., 1977).

The relationship of Bristol Bay winds to the larger scheme of Pacific northern hemisphere air circulation can be seen in the long term (36 year) monthly averages of sea level pressure (Figure 4). Cyclogenesis starts the winter cycle in September in the western Gulf of Alaska, forming the Aleutian Low which rapidly deepens during November and December. This is the time when northeast winds are most probable in Bristol Bay. Northeast winds continue to dominate but are interrupted occasionally by southerly winds as the main low center migrates southwestward and enlarges in January-February. Then, as the Northeast Pacific High enlarges and pushes the Aleutian Low into the central Bering Sea by Spring, the tendency for southwest winds in Bristol Bay increases, becoming fully developed in July-August coincident with the summer precipitation maximum.

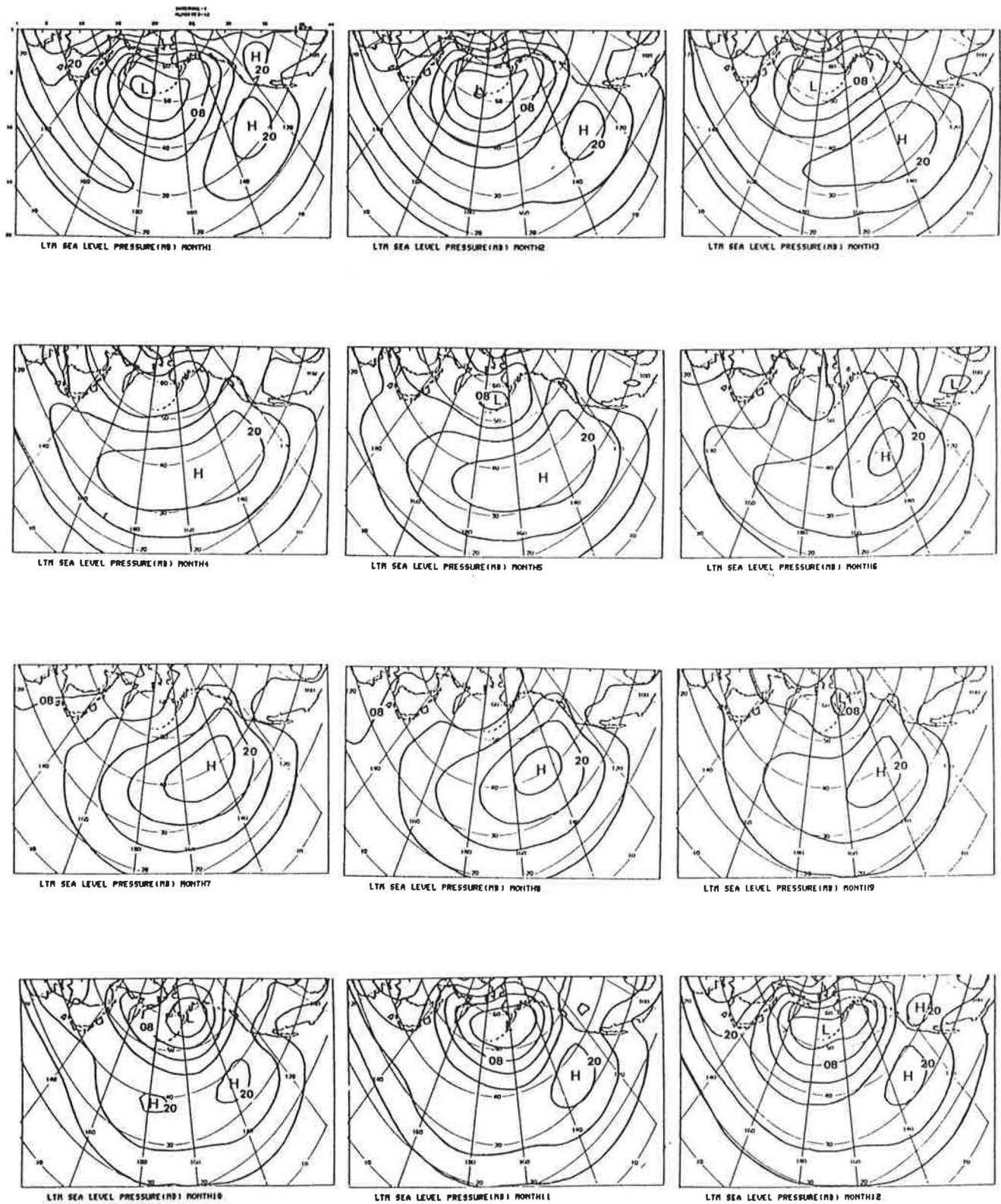


Figure 4.--Long term mean (LTM) sea level pressure -1000(mb) fields by month.

### Bathymetry

The bathymetry of the Southeastern Bering Sea is characterized by a few highly irregular channels and ridges superimposed on an extremely broad gently sloping continental shelf (Figure 5). The most distinct features are the two troughs originating from the bays of the Kuskokwim and Kvichak rivers. The Kvichak trough, the most prominent one, lies alongside the Alaskan Peninsula while the Kuskokwim trough extends southward alongside Cape Newenham.

Along the Alaskan Peninsula depths of 20 m occur very close to shore, the exception being in the bays of Port Heiden and Port Moller where the depths do not exceed 15 m.

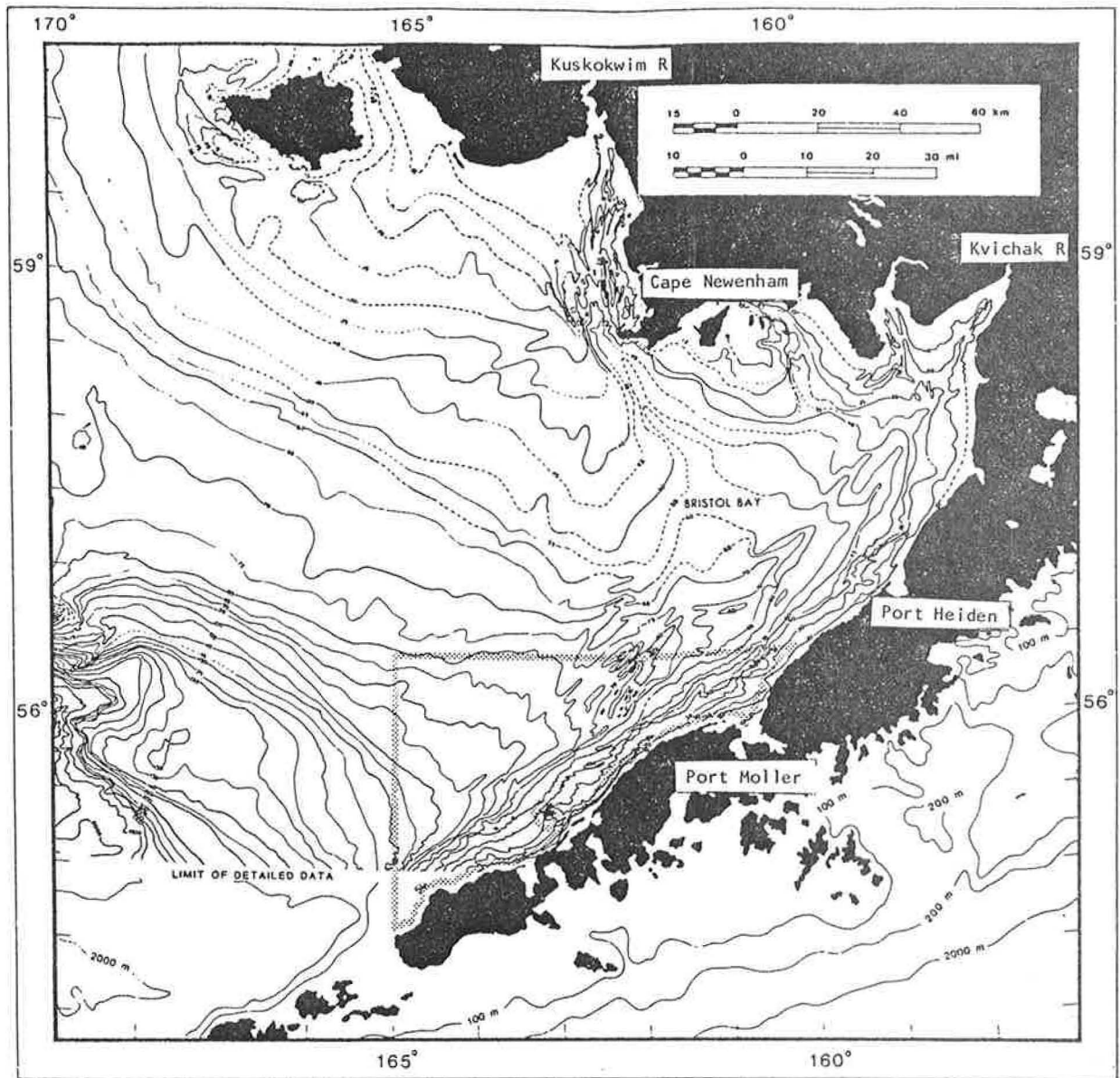


Figure 5.--Bathymetry (m) of the southern Bering Sea shelf.

### Sediments

The great majority of the surficial sediments on the Bristol Bay shelf are sand with varying mixtures of silt, clay, and gravel (Sharma, 1979). Mean grain size decreases offshore (Figure 6) as water depth increases. The coarse to very coarse sands near shore are extremely poorly sorted, the medium and fine sands of the middle shelf are moderately well sorted, and as silt and clay components increase in the outer shelf sorting becomes poor again (Figure 7). The dominance of sand is quantitatively illustrated in the weight percent distributions of silt and clay (Figure 8) which are minimal (1 to 3%) on the middle shelf and increase to 40% and 10%, respectively on the outer shelf. Organic carbon content of sediments (0.05 to 0.55%) increases with increasing clay content (Figure 9).

In examining plots of sediment mean size versus water depth Sharma (1979) showed the inner and outer shelf could be distinguished based on sediment size (Figure 10). The inner shelf < 60 m depth was covered with sediments coarser than  $3 \phi$  while the outer shelf > 75 m depth was mantled only with sediments finer than  $3 \phi$ . The transition zone (60 to 75 m depth) contained both coarser and finer sediments as well significant changes in sorting and skewness. Although there appears to be a general directional agreement, this zonation of sediment size on the shelf does not strictly adhere to the well established hydrographic fronts at 50 and 100 m.

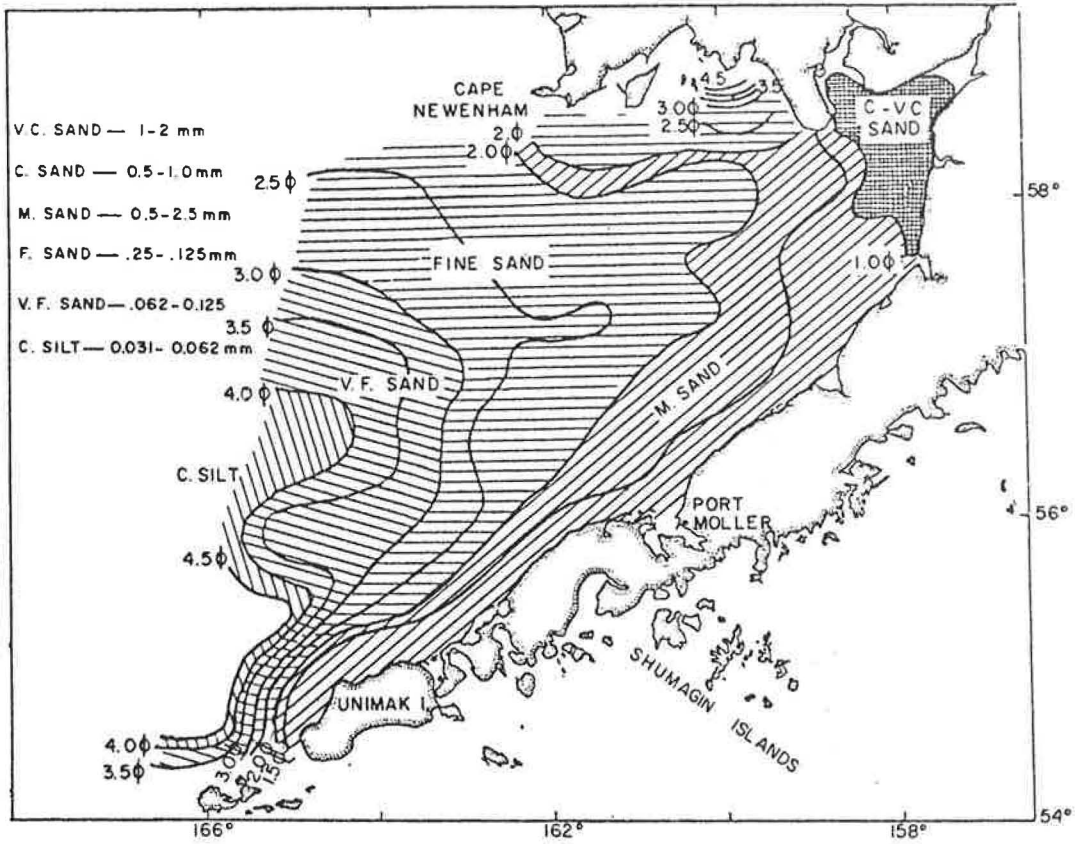


Figure 6.--Sediment mean size distribution (Sharma, 1979).

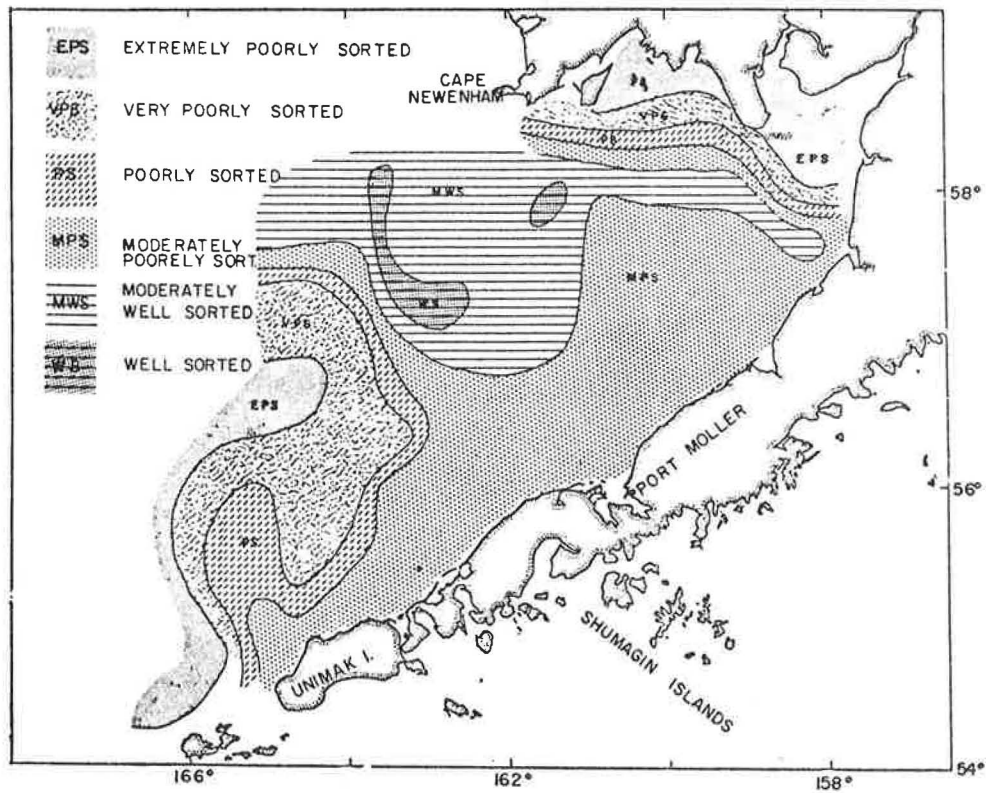


Figure 7.--Grain size sorting (Sharma, 1979).

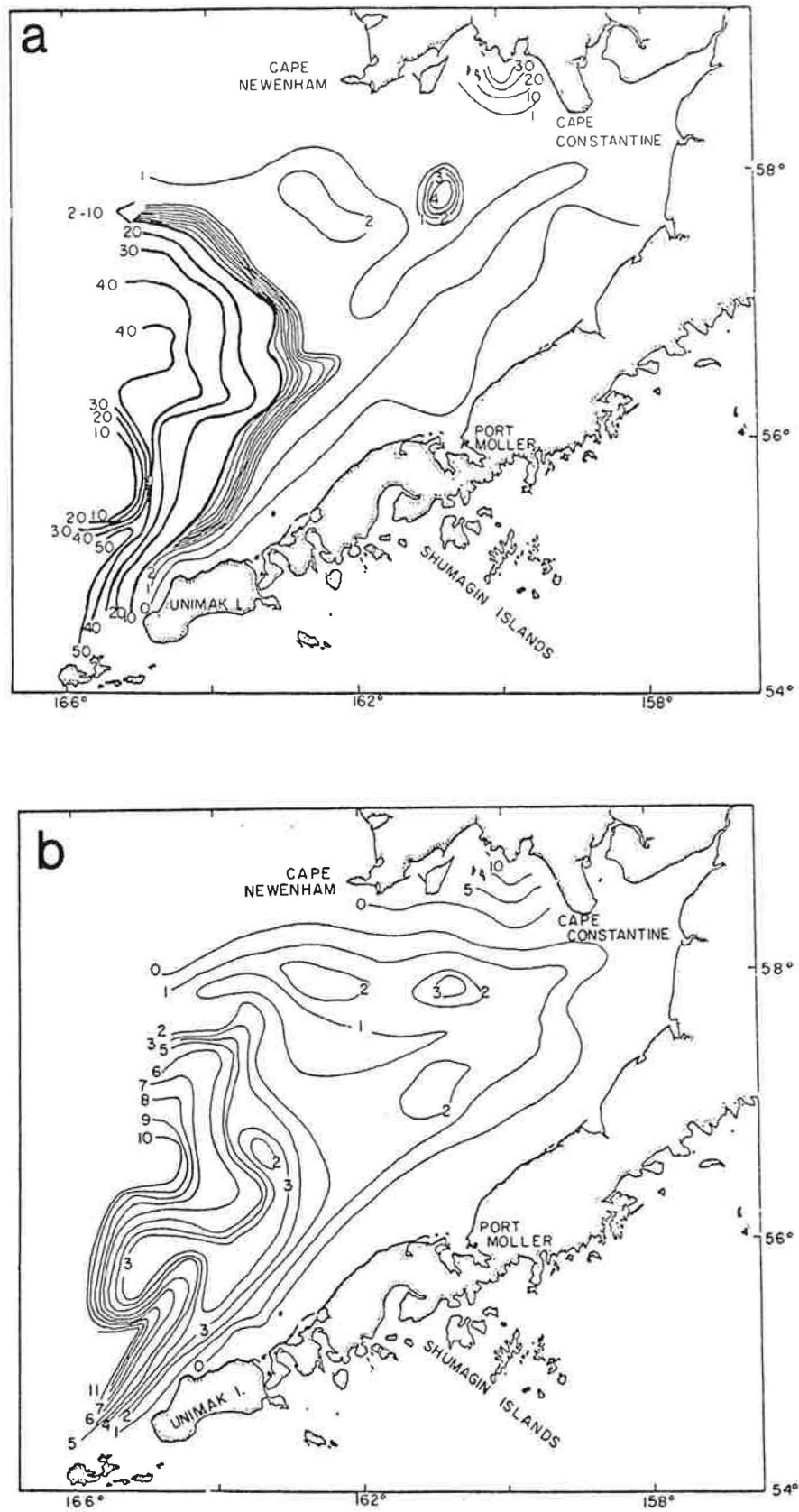


Figure 8.--Weight percent in sediment (a) Silt, (b) Clay (Sharma, 1979).

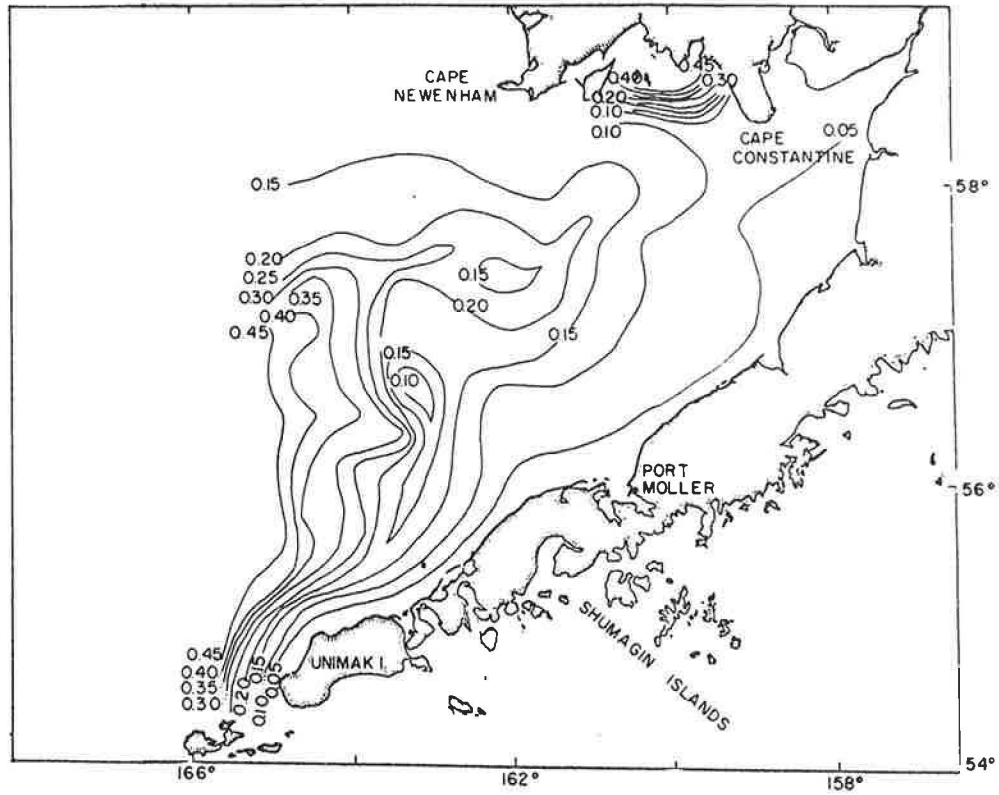


Figure 9.--Weight percent organic carbon in sediments (Sharma, 1979).

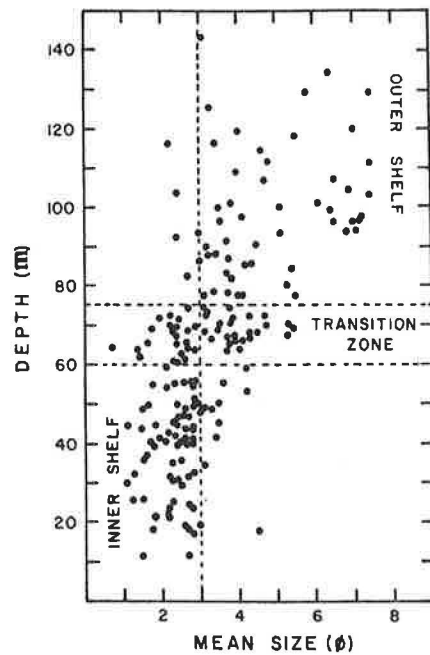


Figure 10.--Water depth (m) versus sediment size ( $\phi$ ) for the Bering Shelf (Sharma, 1979)

### Suspended Particulate Matter

The major source of suspended sediments in the Bristol Bay area is the Kuskokwim River which supplies four million metric tons per year; but contributions from lesser sources such as the Kvichak, Nushagak, or the Wood rivers are unknown, and no estimate has been made for coastal erosion as a secondary sediment source. Concentrations in any of these rivers can reach 500-2000 mg/l in suspensions (Sharma 1979). Although early studies have shown that these high concentrations in rivers decrease sharply in the coastal zone to <10 mg/l and decrease again to <1 mg/l about 75 km seaward of the Alaska Peninsula (Sharma 1979 and Feeley et al. 1981), their quantitative samples have been of limited extent or too broadly spaced to show the important details in the vertical distribution of suspended particulate matter that were later shown by Baker (1983).

Relative importance of Bristol Bay rivers was semi-quantitatively evaluated by Sharma (1979), using the horizontal distribution of surface sediment plumes on density sliced ERTS-1 imagery after the time of the secondary river runoff peak of August and September (Figure 15). Imagery (isodensity distribution of reflectance) on 15 October 1973 shows three prominent sediment sources in inner Bristol Bay (Figure 11a): (1) Port Heiden where the sediment plume from the harbor extends northeastward along the shore, (2) Kvichak Bay where the sediment plume from the Kvichak River extends westward along the north coast, and (3) Nushagak Bay where the plume fills most of the bay, particularly the western side, then disperses westward into Togiak Bay. Imagery on 5 November 1973 (Figure 11b) shows the plume from Togiak Bay extending westward around Cape Newenham, two plumes from the mouth of the Kuskokwim River extending southwestward and southeastward along the shorelines on each side of Kuskokwim Bay, and the most striking feature is a third and

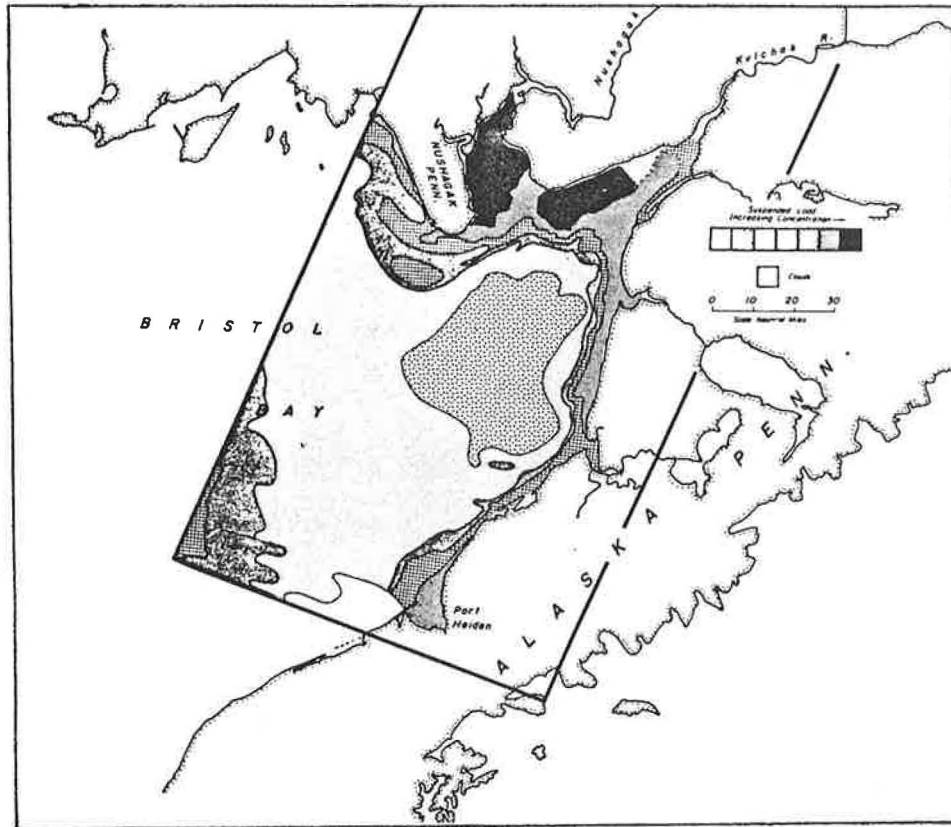


Figure 11a.--Satellite imagery showing relative suspended load in near-surface waters on October 15, 1973 (Sharma, 1979).

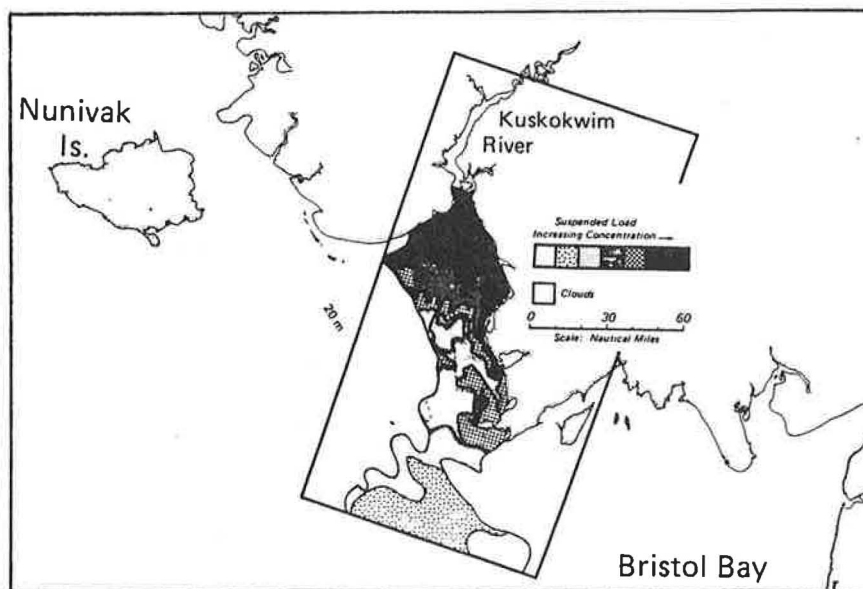


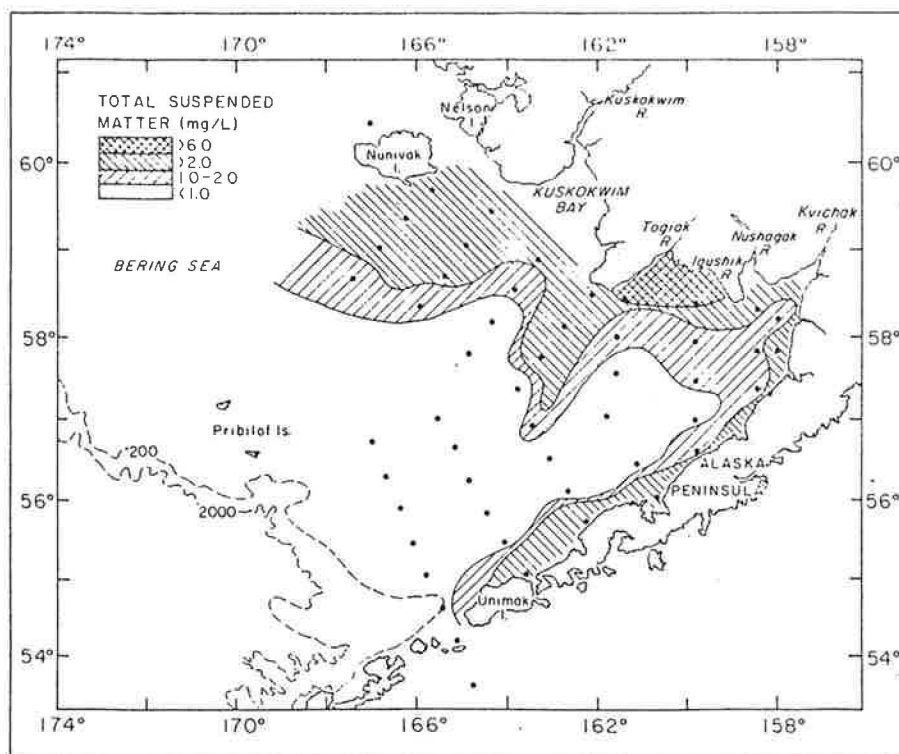
Figure 11b.--Satellite imagery showing relative suspended load in near-surface waters on November 5, 1983 (Sharma, 1979).

broader plume from Kuskokwim Bay extending seaward beyond the coastal zone. Direct measurements, although they were too widely spaced to give details, generally confirmed the features seen in the imagery. Concentrations in the offshore Kuskokwim plume reached 2.2 mg/l in a background of samples generally <1 mg/l outside the plume. Measurements at depth (50-75 m) showed slightly higher concentrations of 2.5 mg/l further westward under the plume. Measurements made near bottom in the coastal zone indicated a two to three fold increase in suspended sediment load during storms due to resuspension.

Additional quantitative measurements of total suspended matter were obtained in Bristol Bay during September-October, 1975 and June-July 1976 by Feeley et al. (1981). These fall surface data (Figure 12a) showed a large plume of suspended matter extending southward from Kuskokwim Bay and a rapid decrease in concentration away from the coast along the Alaska Peninsula confirming the general features discussed by Sharma (1979). The more extensive and detailed data taken near bottom (Figure 12b), however, showed higher than surface concentrations (>1.0 mg/l) throughout the area except for a narrow tongue of less turbid (<1.0 mg/l) water extending into Bristol Bay from offshore just seaward of and parallel to the band of very high concentrations (>2.0 mg/l) in the coastal zone along the Alaska Peninsula.

The latest study (August-September, 1980; January-February, 1981; and May-June, 1981) sampled in great detail both horizontally and vertically along the north coast of the Alaska Peninsula using continuous vertical profiling instruments to obtain both water and suspended particulate structure (temperature, salinity, and light attenuation versus depth) at each station (Baker, 1983). This is the first time the vertical distribution of fine-grained particles has been shown directly related to the hydrographic structural domains (defined based on vertical density structure), a relationship reasonable

a



b

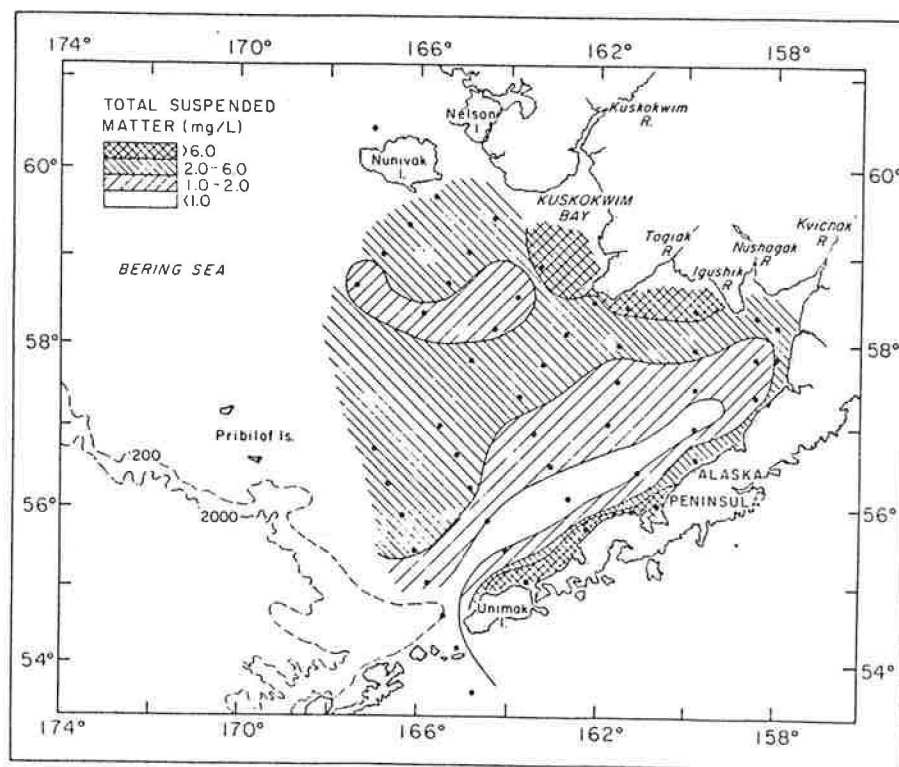


Figure 12.--Distribution of total suspended matter at the surface (a) and 5 meters above the bottom (b) in the southeastern Bering Shelf (cruise RP-4-D: 75-B-III, 12 September - 5 October 1975) (Feely et al. 1981).

to expect because the vertical density structure controls the vertical distribution of turbulence which in turn governs the distribution of particles whose settling velocity is much less than the mean horizontal current. In the coastal domain (about 0-50 m depth) the water properties and particle concentrations are well mixed, as shown in figure 13a by representative vertical profiles of attenuation, Brunt-Vaisala frequency (stability), and  $\sigma_t$  (density). Although the vertical profiles are consistently well mixed, a strong horizontal gradient is present in the coastal domain with particle concentrations decreasing rapidly off shore. In contrast the mid-shelf domain (about 50-100 m depth) has very little horizontal change and a strong vertical structure, two layers in density and three layers in particle concentration (Figure 13b). In the upper, low density layer suspended particle concentrations are a maximum at the surface then decrease to a minimum layer between 30 and 45 m depth. The strong pycnocline near 50 m puts a diffusive lid on the lower, high density layer thus limiting the upward spread of the higher concentrations of resuspended particles near the bottom due to the consistently strong tidal currents. These same features are seen in the outer-shelf domain (Figure 13c) except the pycnocline has expanded over a greater depth range (50 to 70 m) creating a relatively high stability third layer in the water structure.

Seasonal changes and local variability in these major structural features can be seen in vertical cross-sections normal to the coastline seaward of Port Moller during August, 1980, January, 1981, and May, 1981 (Figure 14a, b, and c). Conditions during summer (Figure 14a) showed a weak two-layer density structure with a pycnocline separating the shallow (<about 40 m), turbid, well mixed coastal water from the deeper (> about 50 m) water with the typical three-layer structure of particulate matter. A distinct minimum concentration

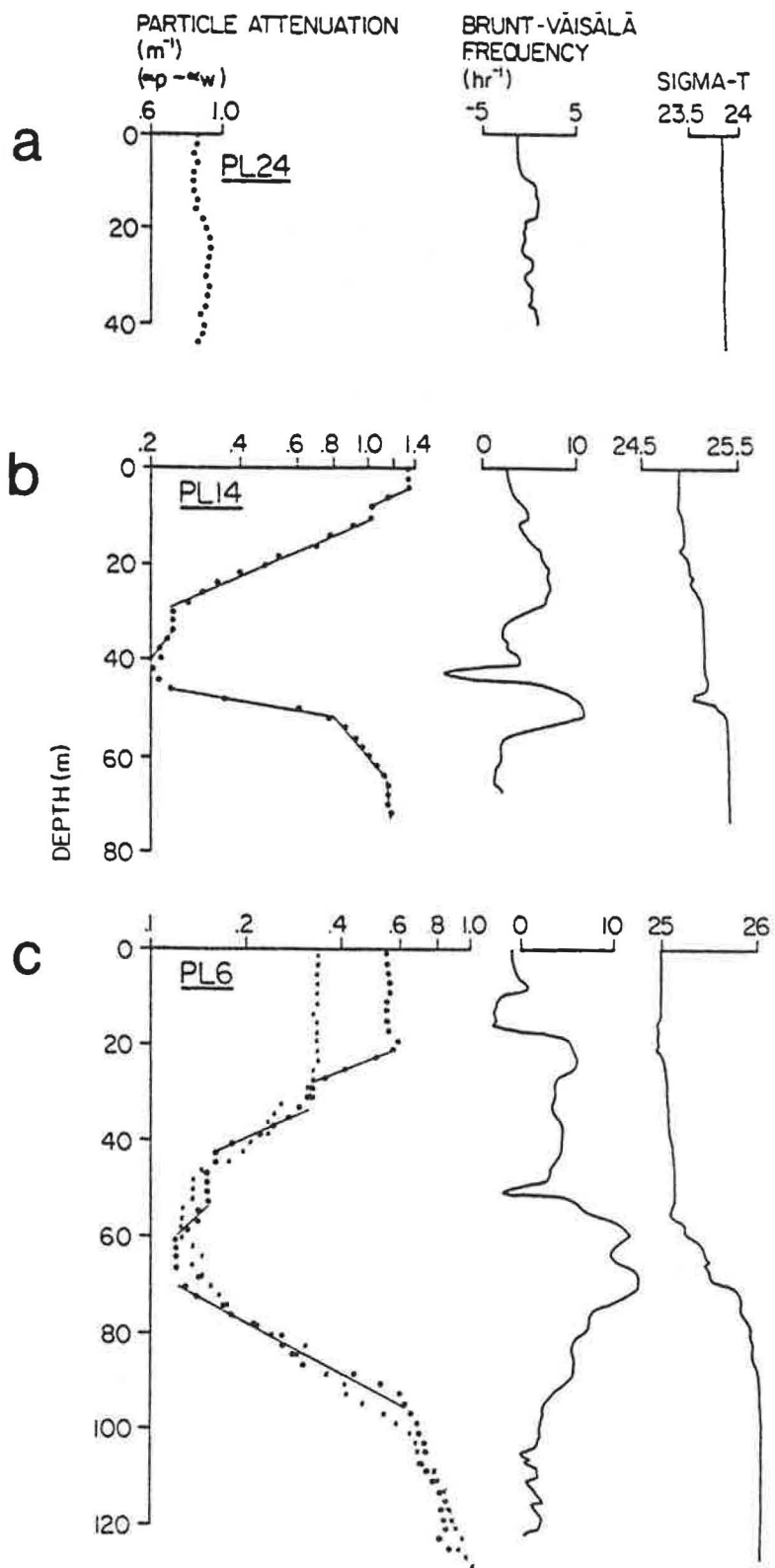


Figure 13.--Net particulate attenuation profiles, stability profiles, and density profiles from the (a) coastal (b) middle and (c) outer-shelf domains (Baker, 1983).

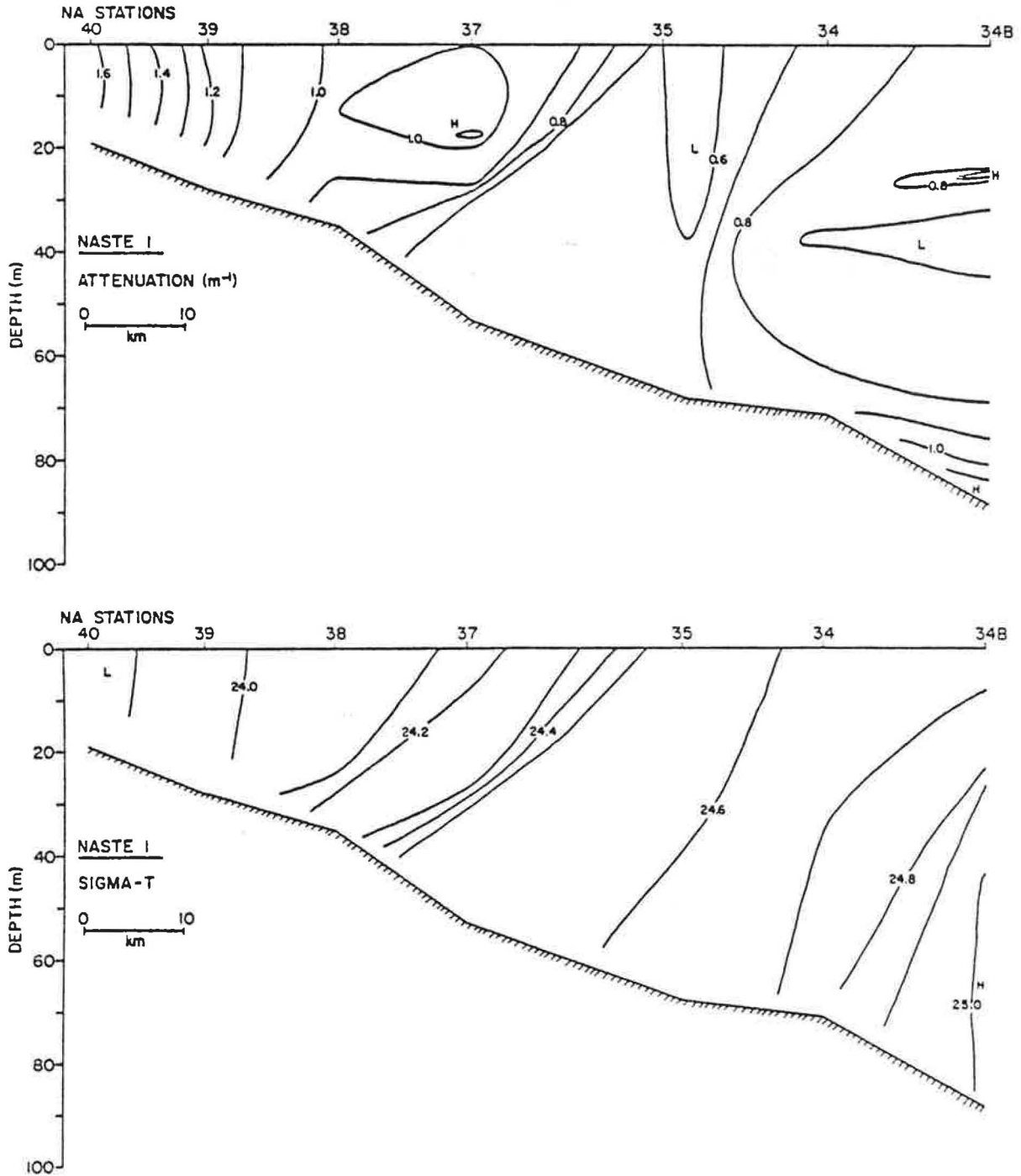


Figure 14a.--Attenuation (top) and density (bottom) cross-sections for line 2 (station NA 34-40), August 1980.

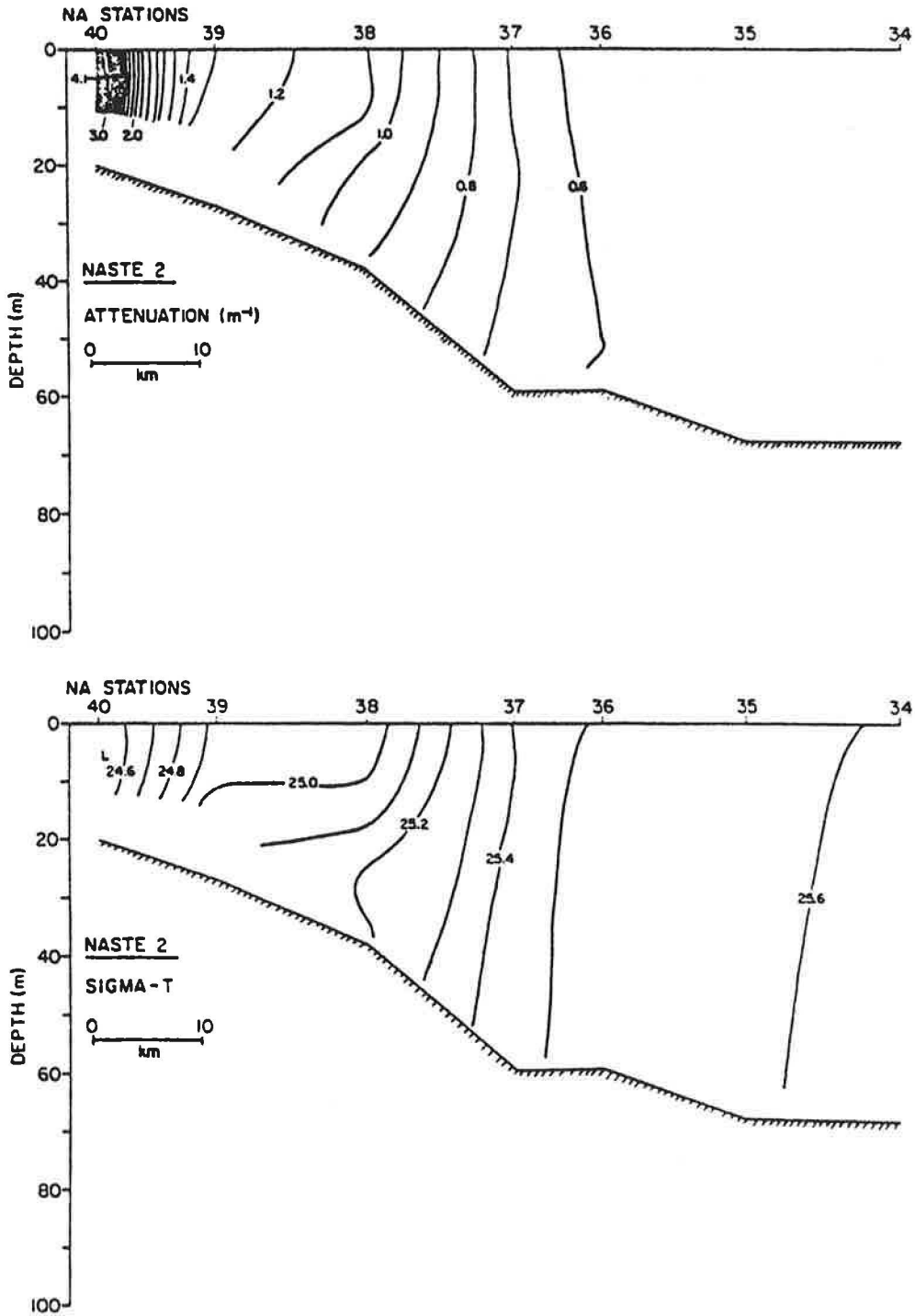


Figure 14b.--Attenuation (top) and density (bottom) cross-sections for line 2 (station NA 34-40), January 1981.

of particulates was evident under the pycnocline along the bottom between about 50 and 60 m. During winter (Figure 14b) conditions changed significantly. Concentrations of particulate matter decreased and density increased seaward in their typical pattern, but mid-shelf domain stratification was essentially absent to at least 80 m depth. Stratification returned during spring (Figure 14c) with isolated maxima in particulates occurring just below the pycnocline and near bottom in the mid-shelf domain. Commensurate with the normal seasonal cycle in biological activity, the organic portion of the suspended particulates ranged from as low as 25% for inshore stations during winter to >50% for offshore surface water samples during spring.

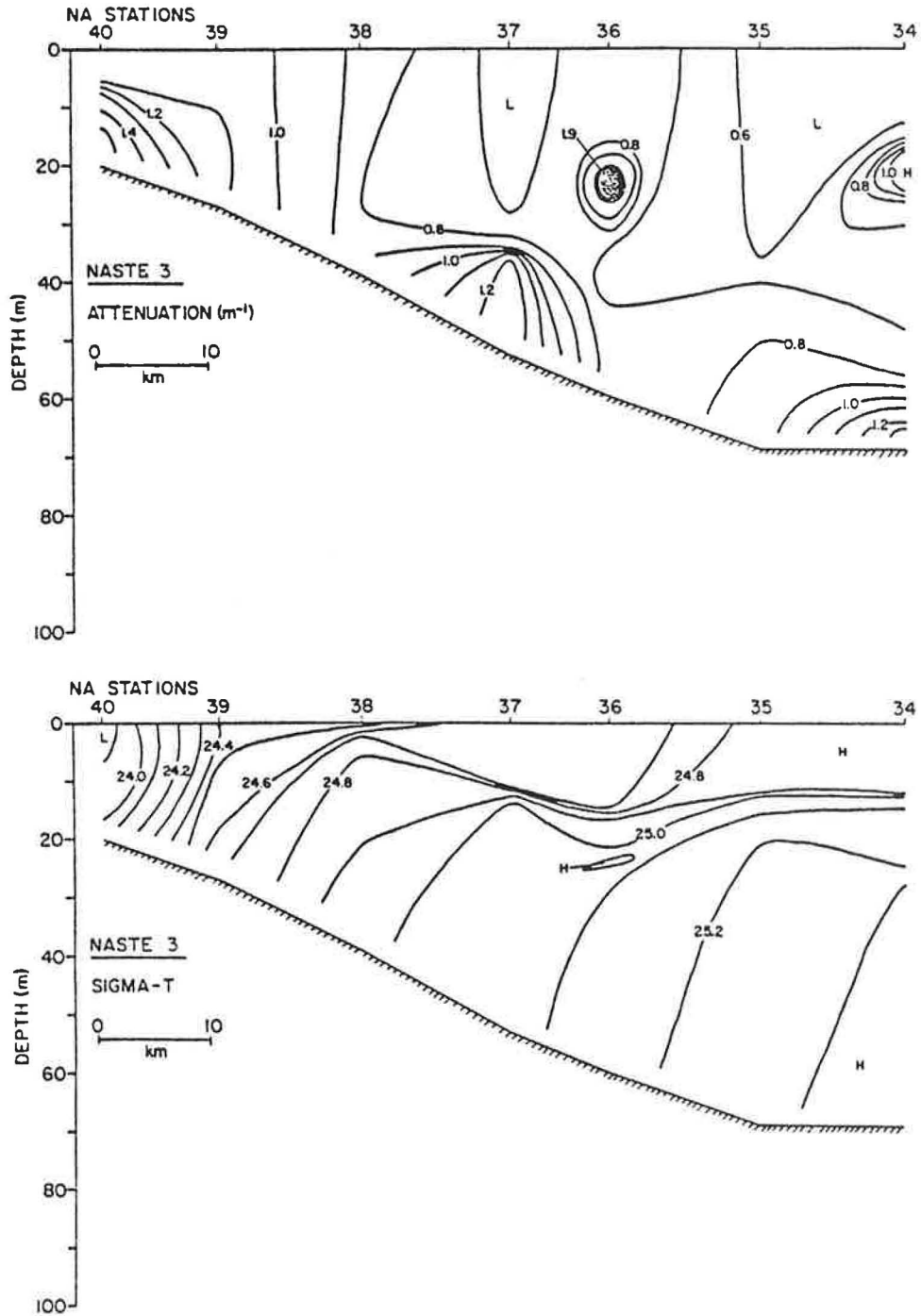


Figure 14c.--Attenuation (top) and density (bottom) cross-sections for line 2 (station NA 34-40), May 1981.

### River Runoff

The largest southeastern Bering Sea river, the Kuskokwim, ranks third with  $990 \text{ m}^3/\text{sec}$  in mean annual fresh water discharge into the Bering Sea (Roden, 1967) after the Yukon River with  $6220 \text{ m}^3/\text{sec}$  and the Anadyr River with  $1660 \text{ m}^3/\text{sec}$ . The following seasonal changes of runoff in the Kuskokwim River also reflect the characteristics of its smaller neighbors around Bristol Bay, the Togiak, Wood, Nushagak, Kvichak, Naknek, Egegik, and Ugashik Rivers. River discharge is consistently low ( $<500 \text{ m}^3/\text{sec}$ ) during the winter ice season from December to April. It is followed by a sharp one month rise to about  $2000 \text{ m}^3/\text{sec}$  during May, then the annual maximum (about  $2700 \text{ m}^3/\text{sec}$ ) in June (Figure 15). This sharp rise is associated with the spring melt during these months. In July a slight relaxation occurs, followed by a secondary maximum during August (about  $2400 \text{ m}^3/\text{sec}$ ) associated with the annual precipitation maximum. September values remain relatively high, but the river discharge declines sharply during October and November, returning the cycle again to its winter low.

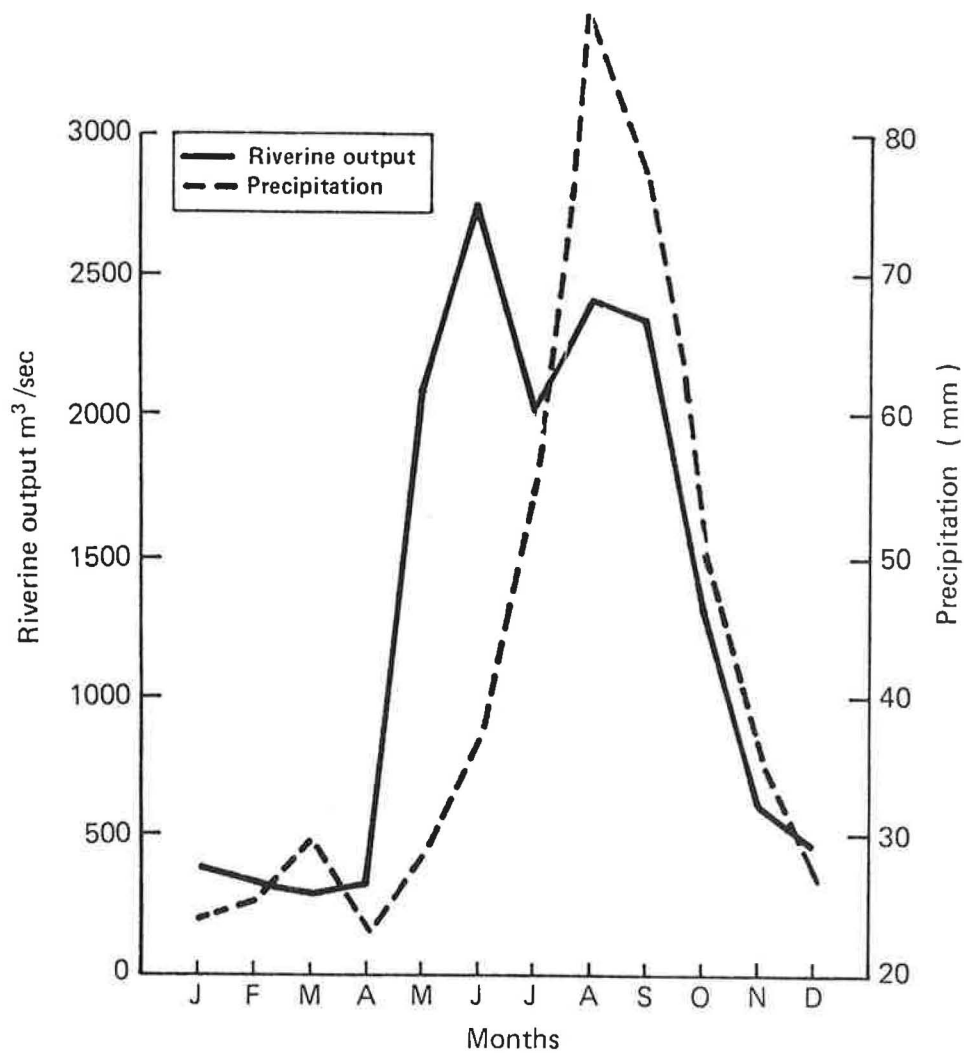


Figure 15.--Average monthly precipitation and riverine runoff for the Kuskokwim River. (Data from Ruffner et. al., 1978 and Roden, 1967).

## Tides

Pressure and current meter data taken during 1975-78 provide new information about tidal heights and tidal currents in the Bristol Bay area (Pearson, Mofjeld, and Tripp, 1981). Cotidal charts prepared from these data show the distribution of tidal coamplitudes (the range in height in cm, dashed lines) and cophase ( $0^\circ$  to  $360^\circ$  referred to Greenwich, solid lines) for the four major tidal components— $M_2$ ,  $N_2$ ,  $K_1$ , and  $O_1$  (Figure 16a, b, c, d). Because the sum of the amplitudes of the semidiurnal components ( $M_2 + N_2$ ) is about twice the sum of the diurnal components ( $K_1 + O_1$ ), the tide type is classified as mixed, predominantly semidiurnal, having two highs and two lows per day and large diurnal inequalities. Offshore in outer Bristol Bay near midshelf amplitudes of all components are small, about 20 to 40 cm. The tidal range then increases greatly toward shore as the water depth shallows. Maximum amplitudes greater than 200 cm occur in inner Bristol Bay embayments where  $M_2$  is about three times larger than  $K_1$ , and  $K_1$  is about twice the nearly equal  $O_1$  and  $N_2$  components. At coastal stations, average predicted diurnal ranges also increase toward inner Bristol Bay, being 330 cm at Port Moller and 689 cm at the Naknek River entrance where the maximum range is expected to be as high as 915 cm (Brower et al., 1977). Cophase lines (Figure 16a, b, c, d) indicate the tide enters the Bering Sea through the Aleutian Island passes and progresses as a free wave along the north side of the Alaska Peninsula into Bristol Bay where it slows and reflects. As the wave passes any one spot, currents change with time with the instantaneous current vector appearing to rotate either clockwise or counterclockwise as viewed from above. This rotation is seen in the ellipse representation of the major components  $M_2$  and  $K_1$  (Figure 17a,b). Ellipses in the figure are centered at the observing station and

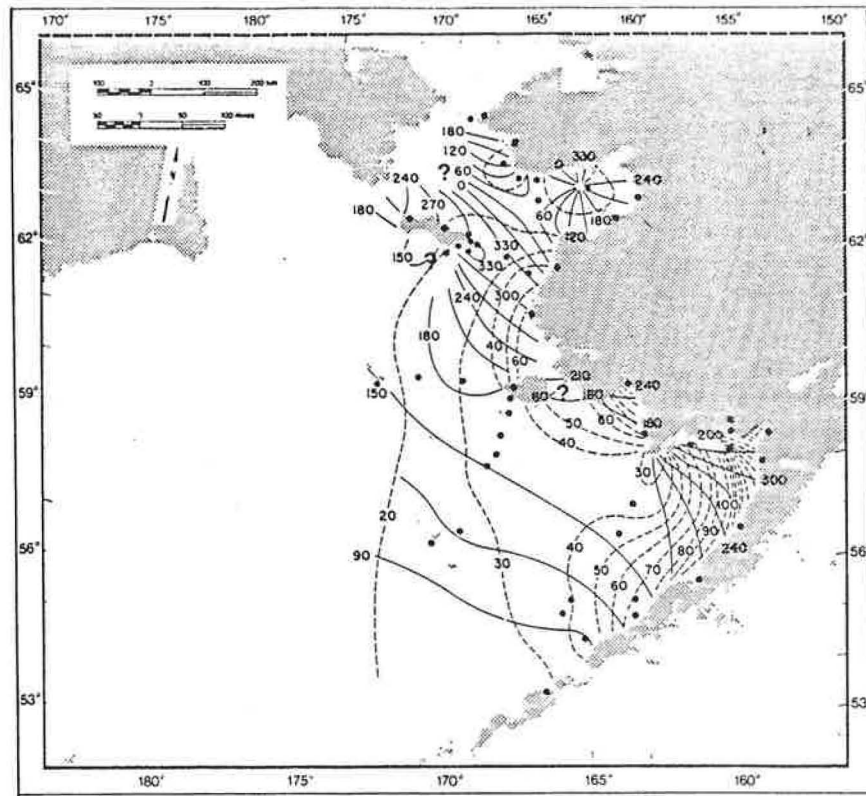


Figure 16a.--Co-tidal chart of the semi-diurnal component  $M_2$ . Dots refer to the stations (Pearson et al., 1981).

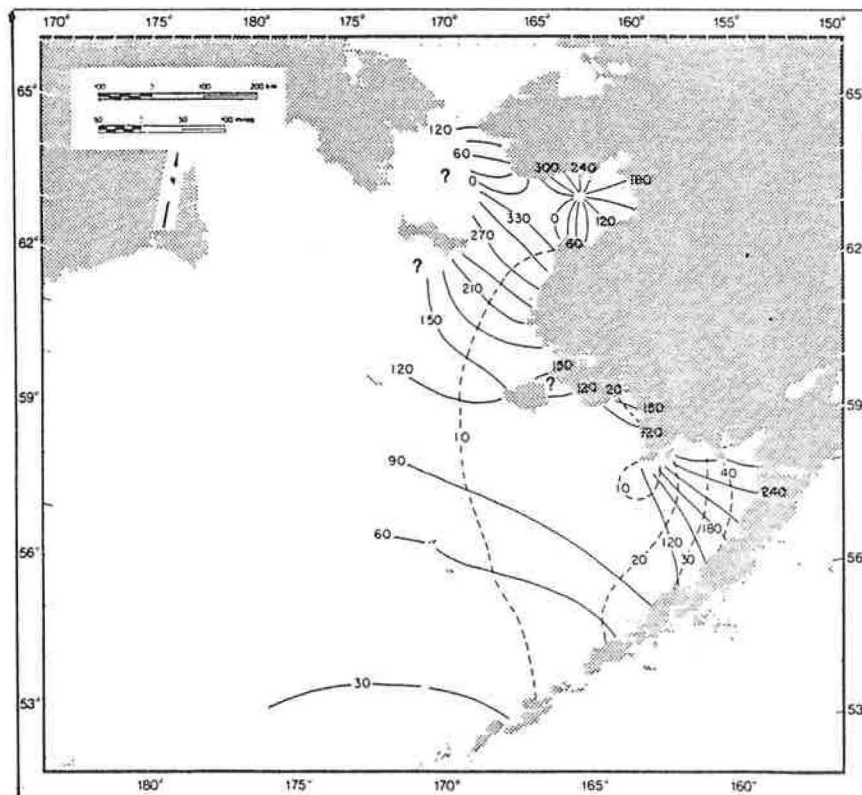


Figure 16b.--Co-tidal chart of the semi-diurnal component  $N_2$  (Pearson et al., 1981).

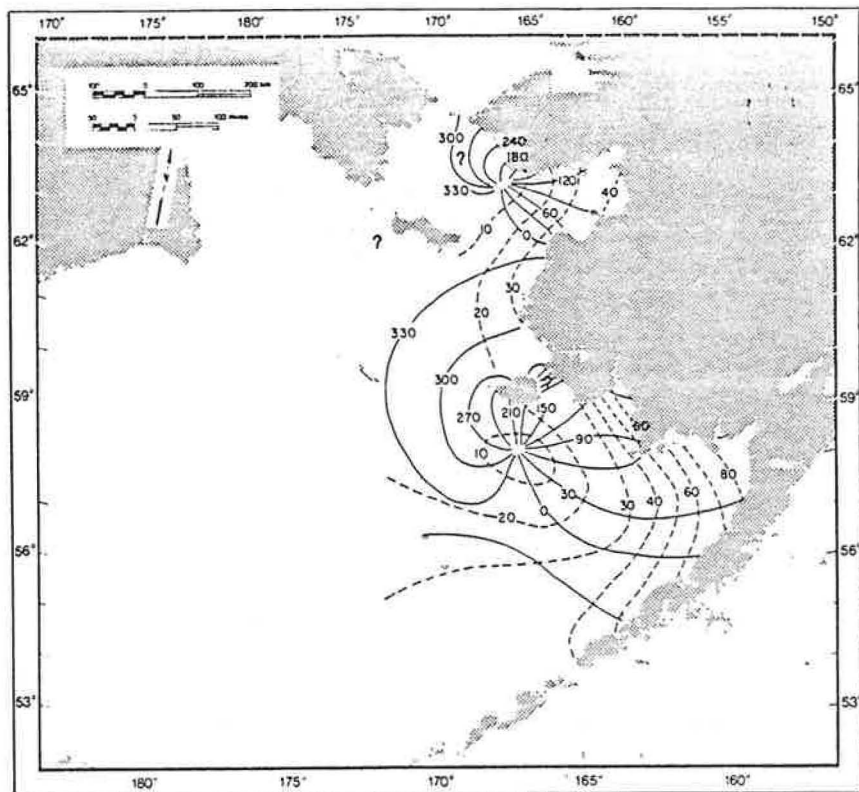


Figure 16c.--Co-tidal chart of the diurnal component  $K_1$  (Pearson et al., 1981).

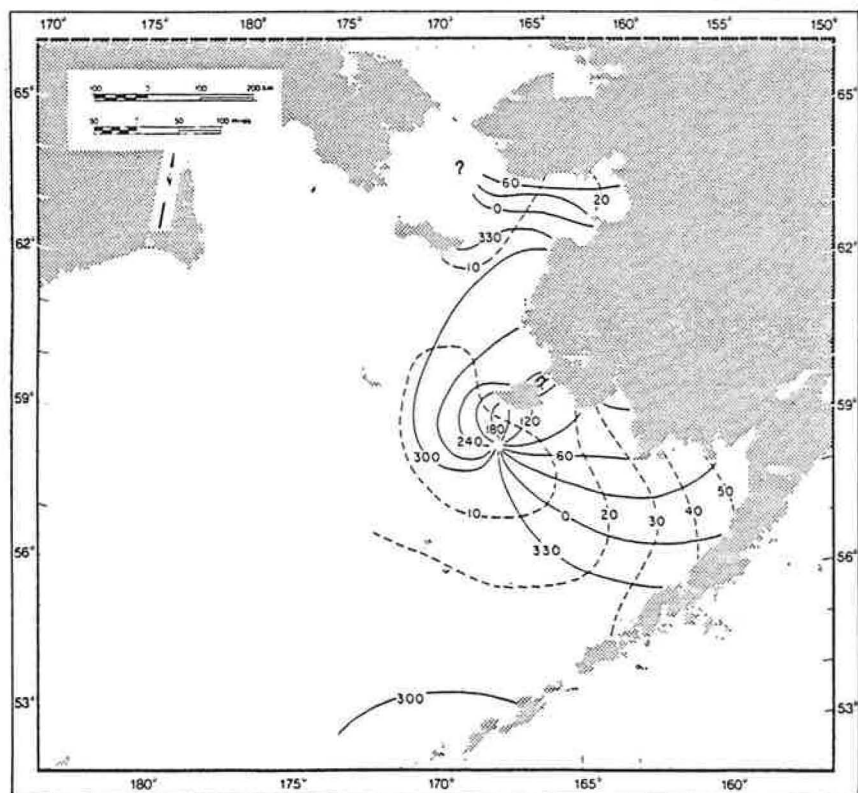


Figure 16d.--Co-tidal chart of the diurnal component  $O_1$  (Pearson et al., 1981).

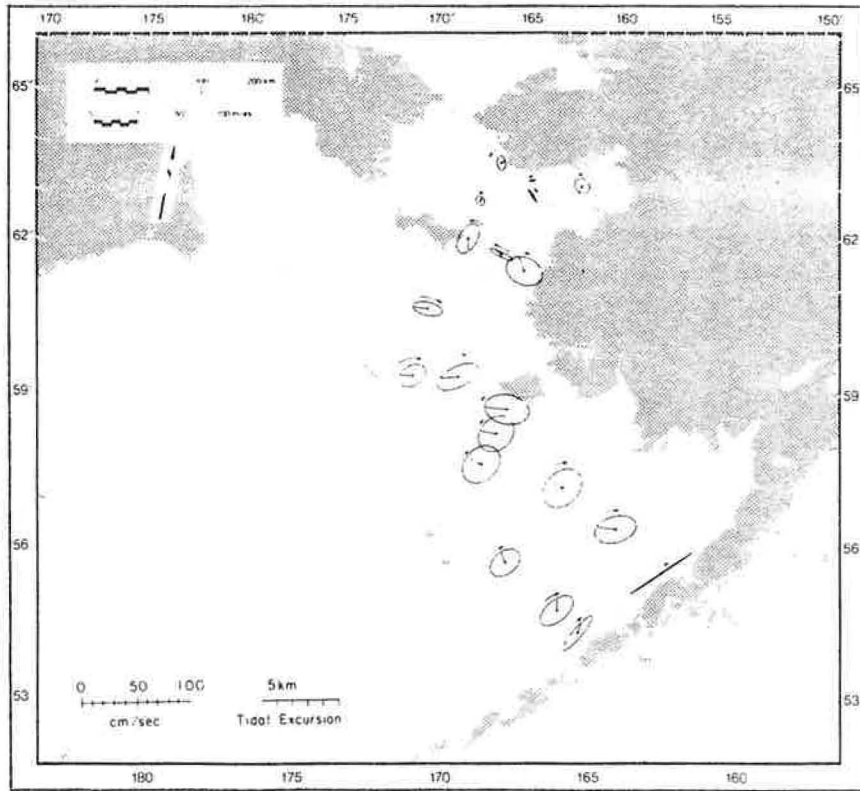


Figure 17a.-- $M_2$  current ellipses (Pearson et al., 1981).

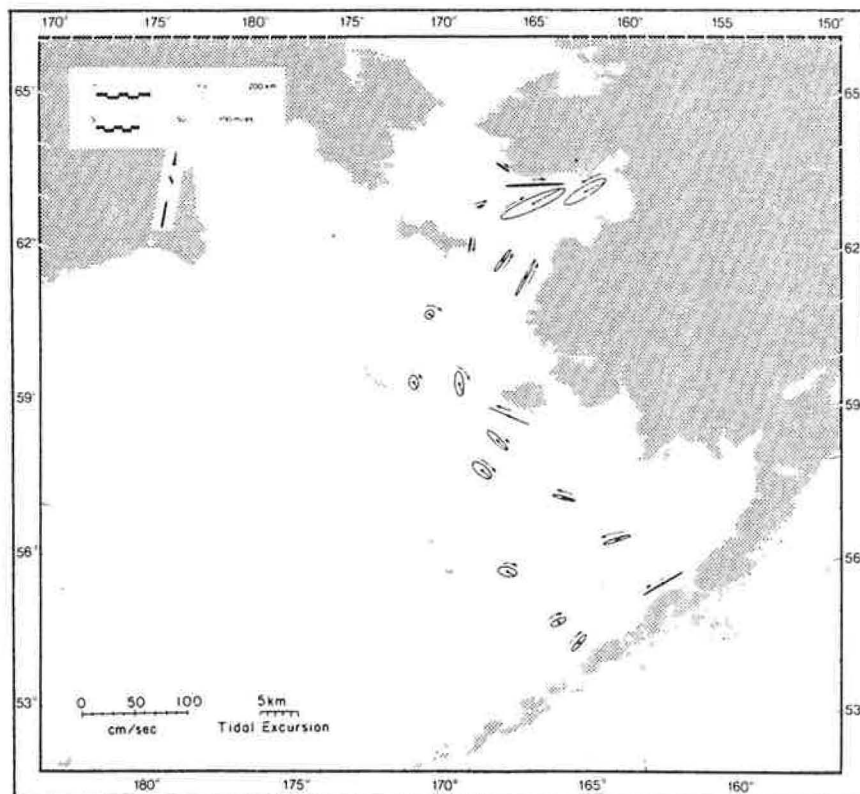


Figure 17b.-- $K_1$  current ellipses (Pearson et al., 1981).

the current vector from the center to the ellipse traces out the amplitude and direction of the current with time. They tend to be more circular away from land with the major axis aligned with the direction of the tidal wave propagation.  $M_2$  rotates clockwise with typical speeds of 15-30 cm/sec throughout Bristol Bay and shows a strong topographic influence, becoming nearly rectilinear north of the Alaska Peninsula. The other semidiurnal component,  $N_2$ , shows similar features but is about 25-40% of  $M_2$ . The  $K_1$  ellipses are narrower than the  $M_2$  ellipses and rotation is counterclockwise, opposite to that of the  $M_2$  ellipses.  $K_1$  flow speeds of 10-20 cm/sec are one third slower and more directionally aligned into and out of Bristol Bay. The secondary diurnal component,  $O_1$ , is similar to  $K_1$  but small in amplitude by 60-75 percent. Although this discussion of the major periodic components gives good insight into the dominant features which are possible in the flow regime, it must be remembered that the actual flow is forced by the sum of all the interactions of these components plus the added effects of wind, bottom topography, and internal density structure. Instantaneous pictures of the flow field can only be simulated by sophisticated numerical models such as those developed by Liu and Leendertse (1979).

### Non-tidal Currents

After the semidiurnal (twice daily) and diurnal (daily) astronomically forced tidal flow which dominated 60 to 90 percent of the total flow energy was filtered out of the current meter data, a low-frequency flow, quasi-periodic at about one week, accounted for the next 3-20 percent and the long term mean flow made up only 1 percent of the total flow energy (Kinder and Schumacher, 1981). Although the mean flows are calculated from vector averages over the individual current meter record lengths which are relatively short (3-7 months) compared to the desired but not available continuous multi-year measurements, there was sufficient data from 1975-78 and enough in each season to compile a general summary.

Three distinct regimes were defined for the Bristol Bay area based upon their mean and wind-driven flow characteristics (Figure 18). The coastal regime, from the shoreline to the 50 m isobath, has a mean current flowing northeastward at 2-5 cm/sec following the local bathymetry of the Alaska Peninsula into Bristol Bay then turns northwestward at 1-3 cm/sec out of Bristol Bay along the Alaskan coast. This flow is augmented by occasional wind-driven pulses of a few days duration. The middle regime, between the 50 and 100 m isobaths, has an extremely weak flow (<1 cm/sec) about the same order of magnitude as the error estimates in the data. Wind-driven pulses appear stronger here than in the coastal regime. The third, or outer regime, beyond the 100 m isobath to the shelf break, has a northwestward mean flow of 1-5 cm/sec parallel to the shelf break and low frequency events associated with variations in the Bering Slope Current rather than related to local winds.

Seasonal changes in flow are expected because winter mean wind speeds are higher, mean wind direction reverses compared to summer, and storms

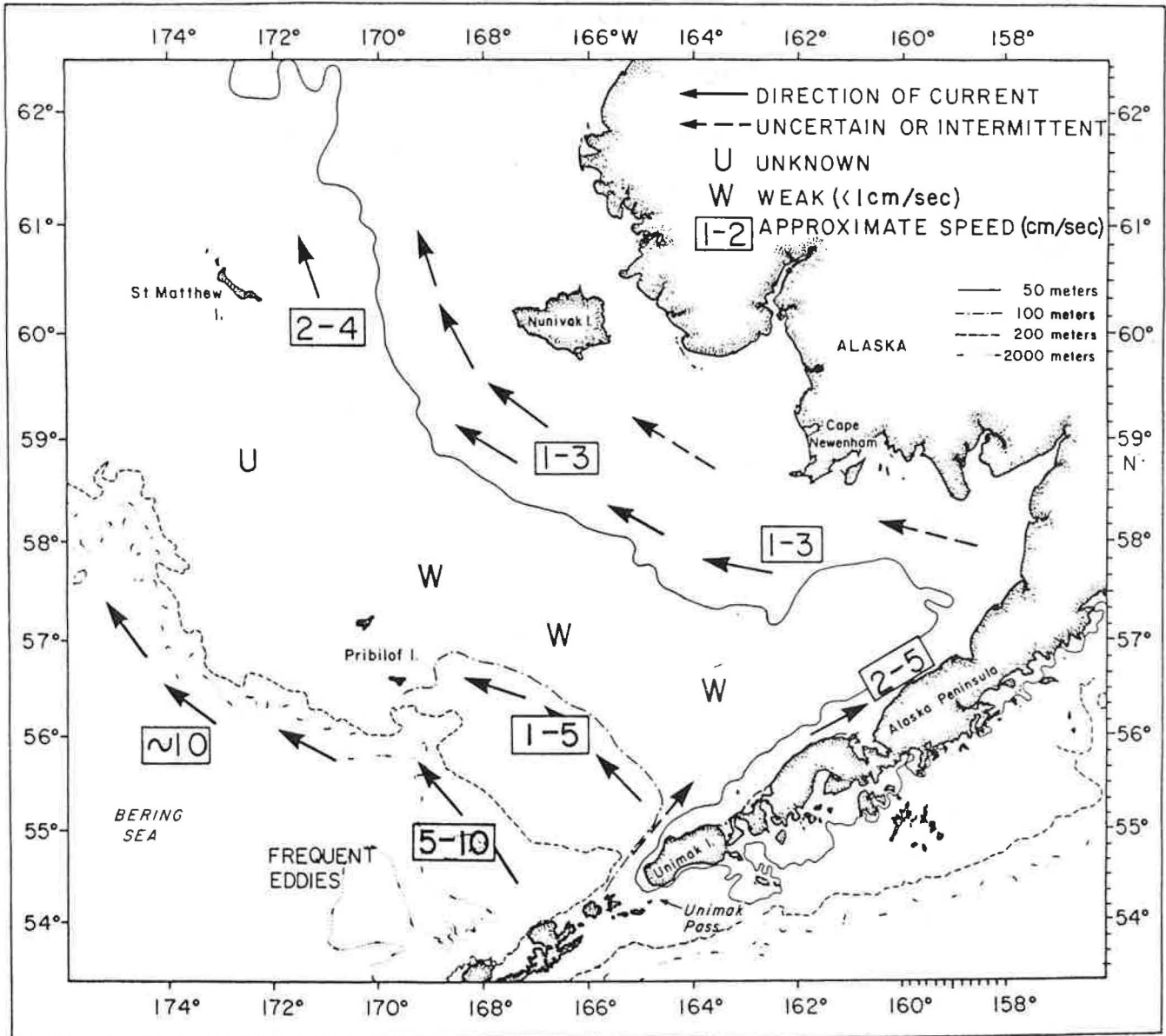


Figure 18.--Mean circulation of Southeastern Bering Sea (Kinder and Shumacher, 1981).

more frequent. Recalling that the above mean flows were measured for periods shorter than one year, their summer-winter change was small but significant. Some data from the coastal regime indicated up to a three-fold increase in mean speed without a change in direction. A two-fold increase in mean speed also occurred in the middle regime of winter, but direction reversed from westward in summer to eastward in winter.

These changes in seasonal mean flow appear related to the cumulative effect of wind forcing from two types of low frequency events. The first type is the eastward-traveling low atmospheric pressure centers which slowly cross the Bristol Bay area mainly during the summer and also occasionally throughout the year. The second type, from large winter low pressure centers in the Gulf of Alaska, is a southward outbreak of cold continental air which frequently produces southerly pulses of surface current at 15-30 cm/sec, lasting 1-5 days. It is suggested that the more complete, meteorological data set be studied for the frequency of these events, thus potentially indicating an index of past interannual variations.

### Water Temperature

Variations of surface temperature are primarily affected by insolation with secondary effects being air temperature, wind speed, river runoff, cloud cover, and precipitation. Monthly means (Figures 19a and 19b) show the effect of insolation, indicating a warming trend starting during the months of April to May, reaching a maximum temperature of over 10°C during August. The cooling period starts during September to October with coastal ice beginning to form during November and ice expansion continuing until March or April (Ingraham, 1981).

Bottom temperatures are affected by vertical circulation and diffusion and the mean horizontal flow. Mean temperatures (Figures 20a and 20b) show that during winter months the thermocline is nonexistent and the isothermal water column approaches the bottom to a depth of about 75 m.

With all temperature measurements there are some interannual variations. Anomalies (Figures 22 and 23) averaged over DYNUMES Areas 1 to 3 (Figure 21), can be over 6°C during any one year, especially in shallow water (less than 30 m).

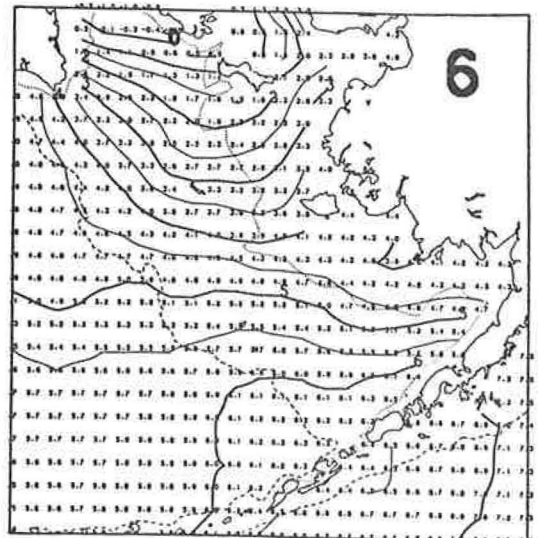
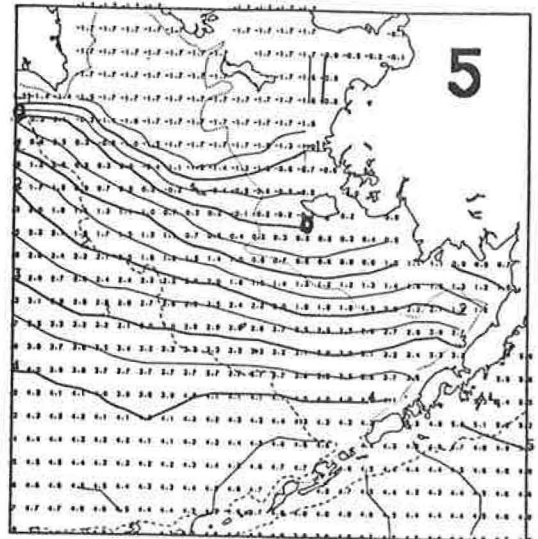
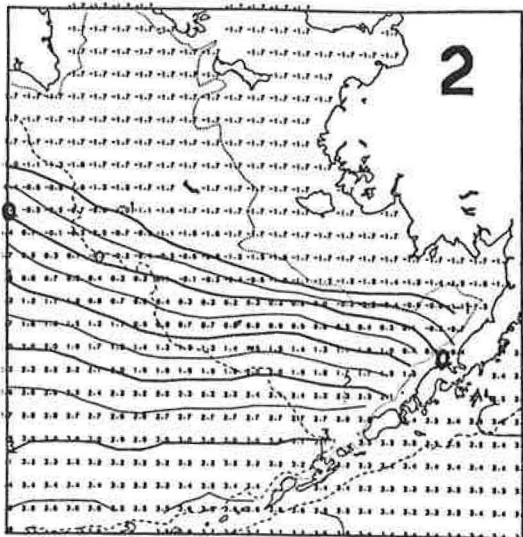
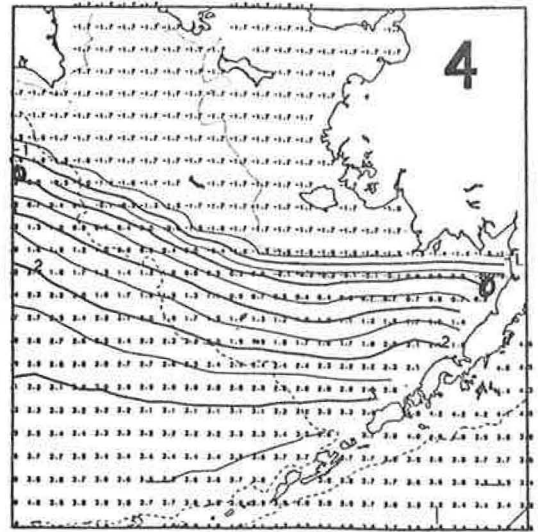
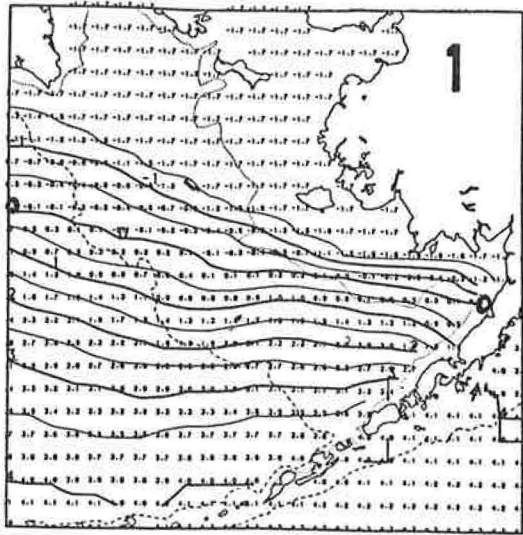


Figure 19a.--Average surface temperatures ( $^{\circ}\text{C}$ ) months 1 to 6.

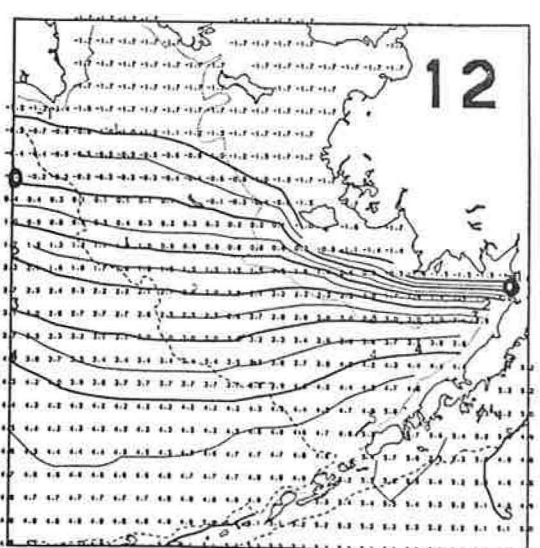
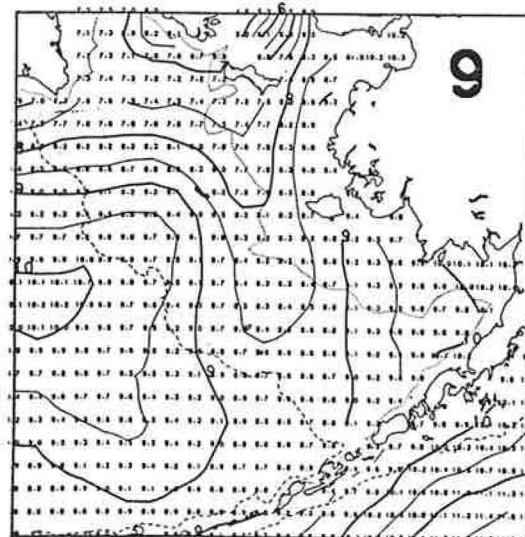
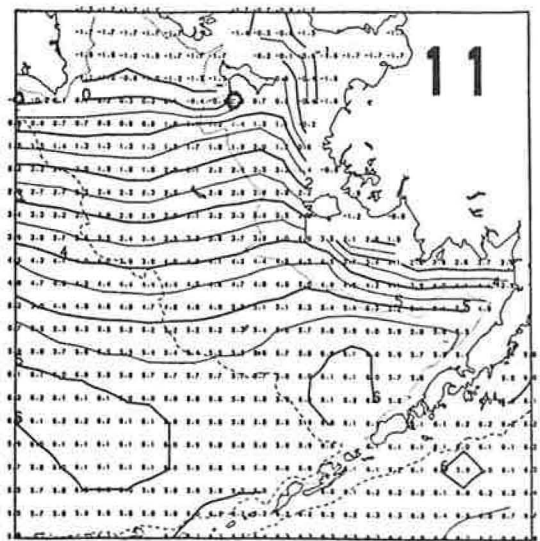
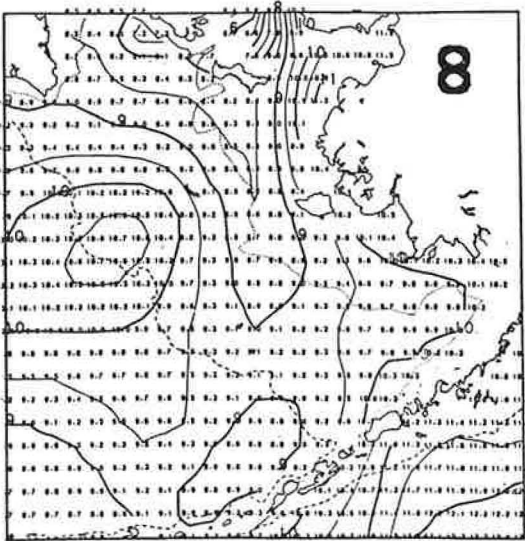
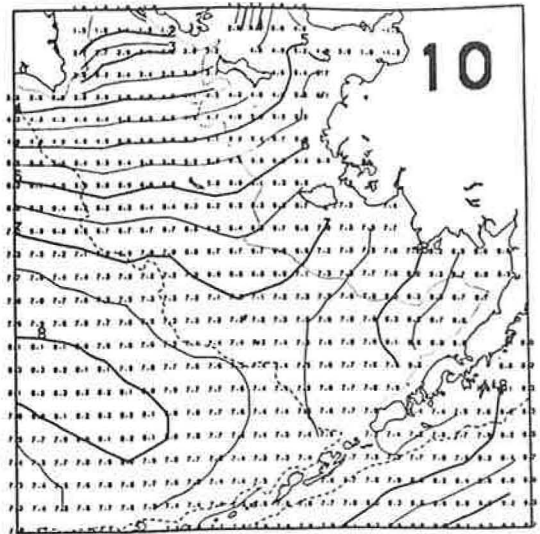
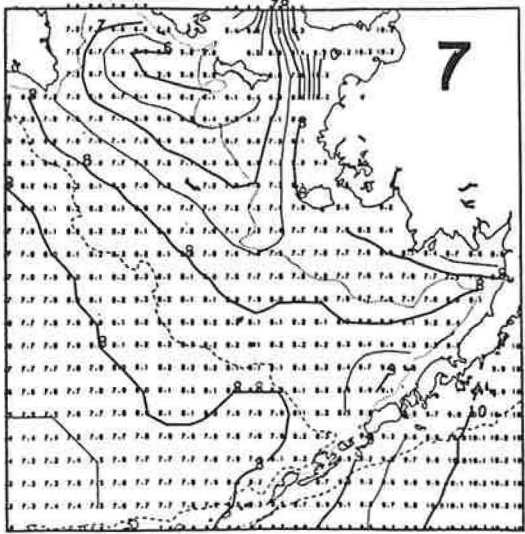


Figure 19b.--Average surface temperatures ( $^{\circ}\text{C}$ ) months 7 to 12.

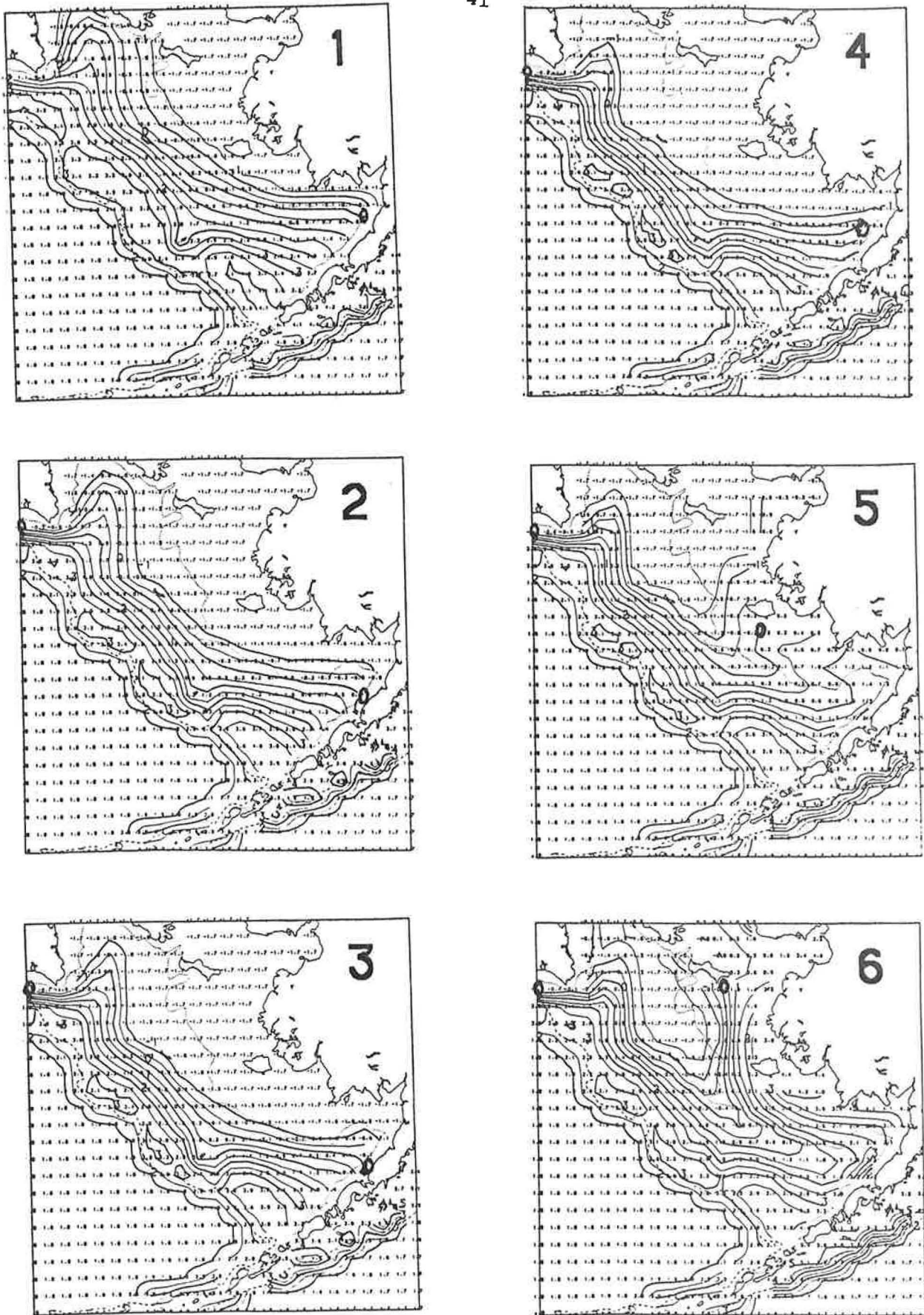


Figure 20a.--Average bottom temperatures ( $^{\circ}\text{C}$ ) months 1 to 6.



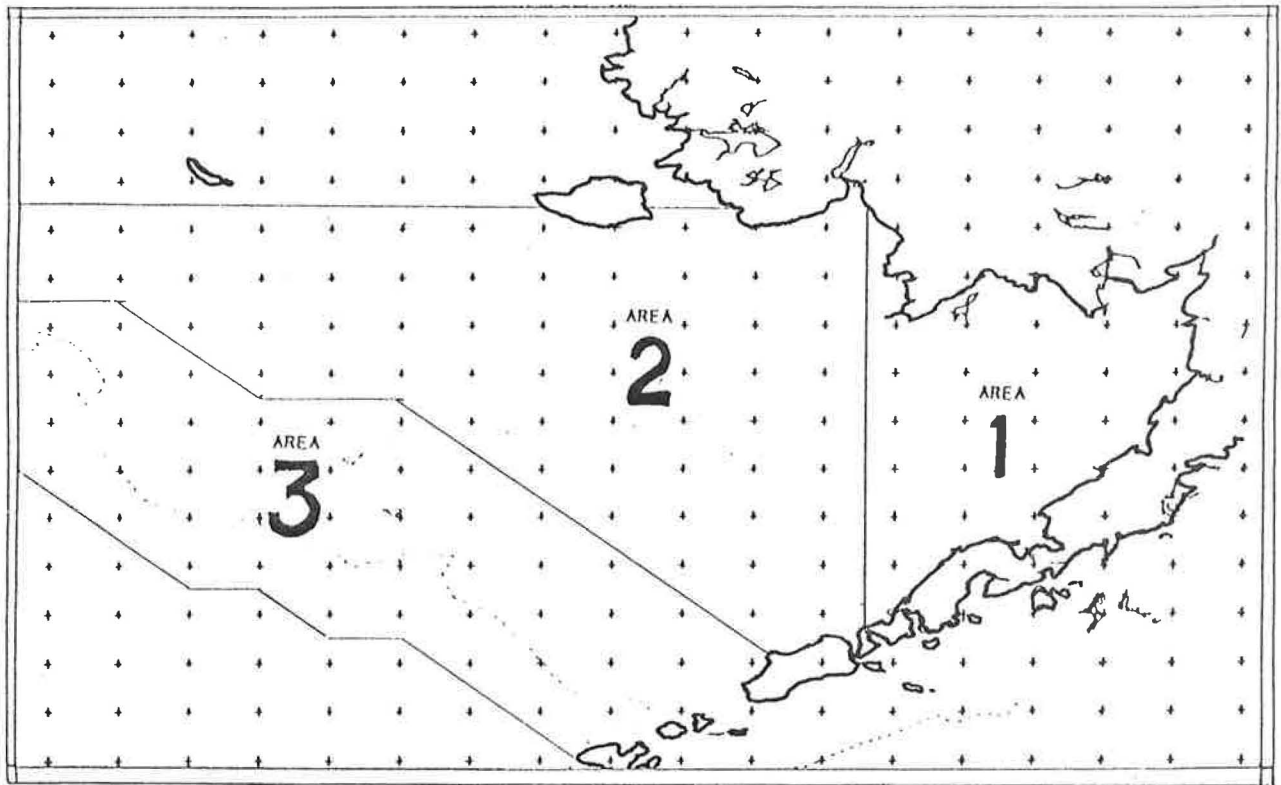
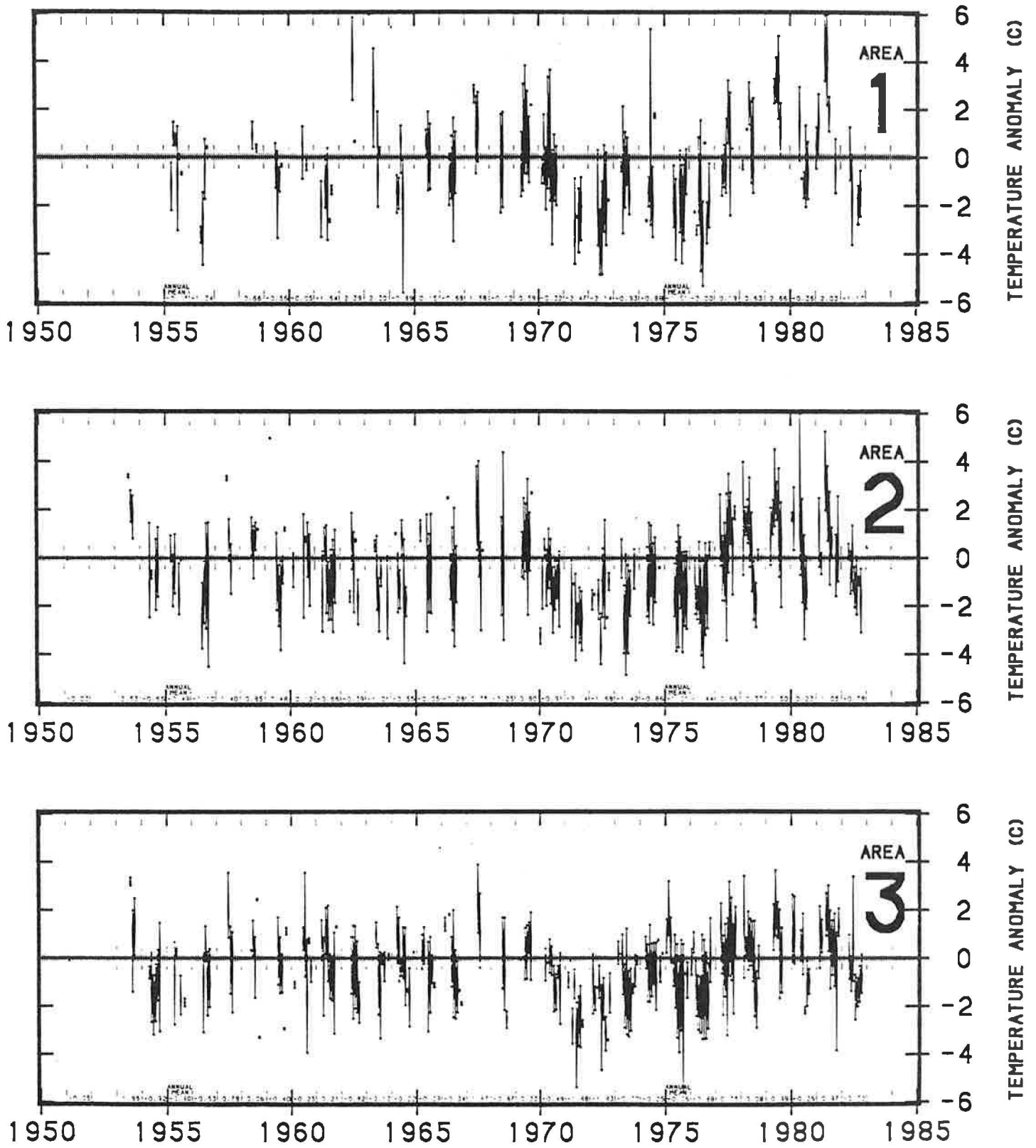


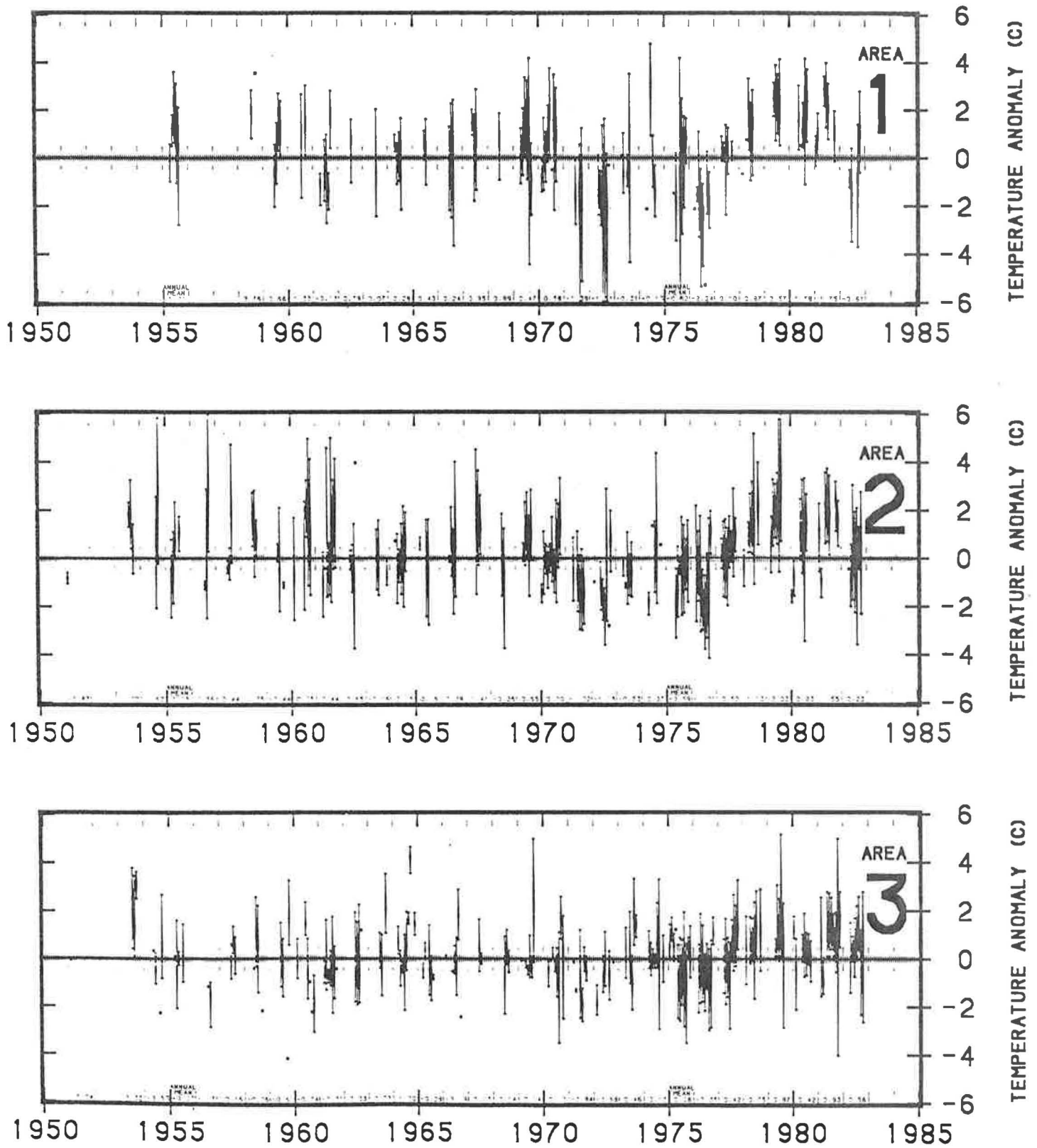
Figure 21,--DYNAMES areas 1 to 3.



MAXIMUM MONTHLY  
AVERAGE MONTHLY  
MINIMUM MONTHLY

BERING SEA SURFACE TEMPERATURE ANOMALIES BY DYNAMES AREAS

Figure 22.--Surface temperature anomalies - DYNAMES areas 1 to 3 (Pola Swan and Ingraham, 1984).



MAXIMUM MONTHLY  
AVERAGE MONTHLY  
MINIMUM MONTHLY

BERING SEA BOTTOM TEMPERATURE ANOMALIES BY DYNAMES AREAS

Figure 23.--Bottom temperature anomalies. DYNAMES areas 1 to 3 (Pola Swan and Ingraham, 1984).

Ice

Ice in the Southeastern Bering Sea occurs when the surface water temperatures reach about  $-1.7^{\circ}\text{C}$ . Because of the differing latitudes (colder toward north) of Cape Newenham, Port Heiden, and Port Moller, the formation of ice occurs at different times. Ice around Cape Newenham forms during November and dissipates during May. Port Heiden and Port Moller ice forms during January and melts during April (Brower et.al.) (Figure 24).

In anomolously warm years, the ice around Ports Heiden and Moller are nonexistent because these ports are usually the southern extent of fast ice. In an extremely cold year (1976), fast ice closes both Ports and extends out along the Alaska Peninsula to half way between Port Moller and Cold Bay.

Sea ice in the Bering Sea is renewed and melts each year. Ice over mid-shelf in the northern part of the Bering Sea appears to be advected southward as winter progresses.

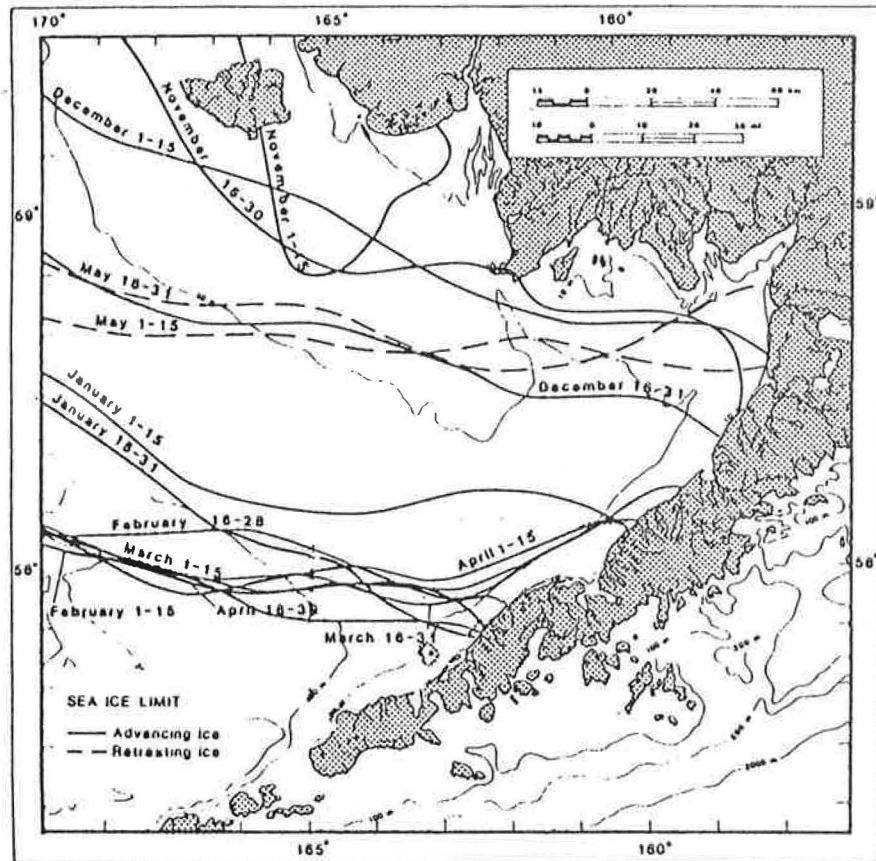


Figure 24.--Approximate ice edge for each month (Brower et al. 1977).

### Salinities

Salinities of the Bering Sea are fairly consistent from season to season with the 33<sup>0</sup>/oo isohaline following the 200 m isobath and the 32<sup>0</sup>/oo isohaline following the 100 m isobath (Ingraham, 1981a) (Figures 25 and 26). There are, however, some local effects which change the salinity by 1<sup>0</sup>/oo or 2<sup>0</sup>/oo. These effects are most prominent in the winter where the increased salinity is due to the lack of riverine outfall, decreased precipitation, and freezing. The most striking effect is salt exclusion during freezing.

During May the spring thaw begins, the riverine runoff increases, and coastal ice melts. These factors will lower the surface salinity during the spring and early summer. Another factor is that the precipitation dramatically increases during August, further diluting the salinity.

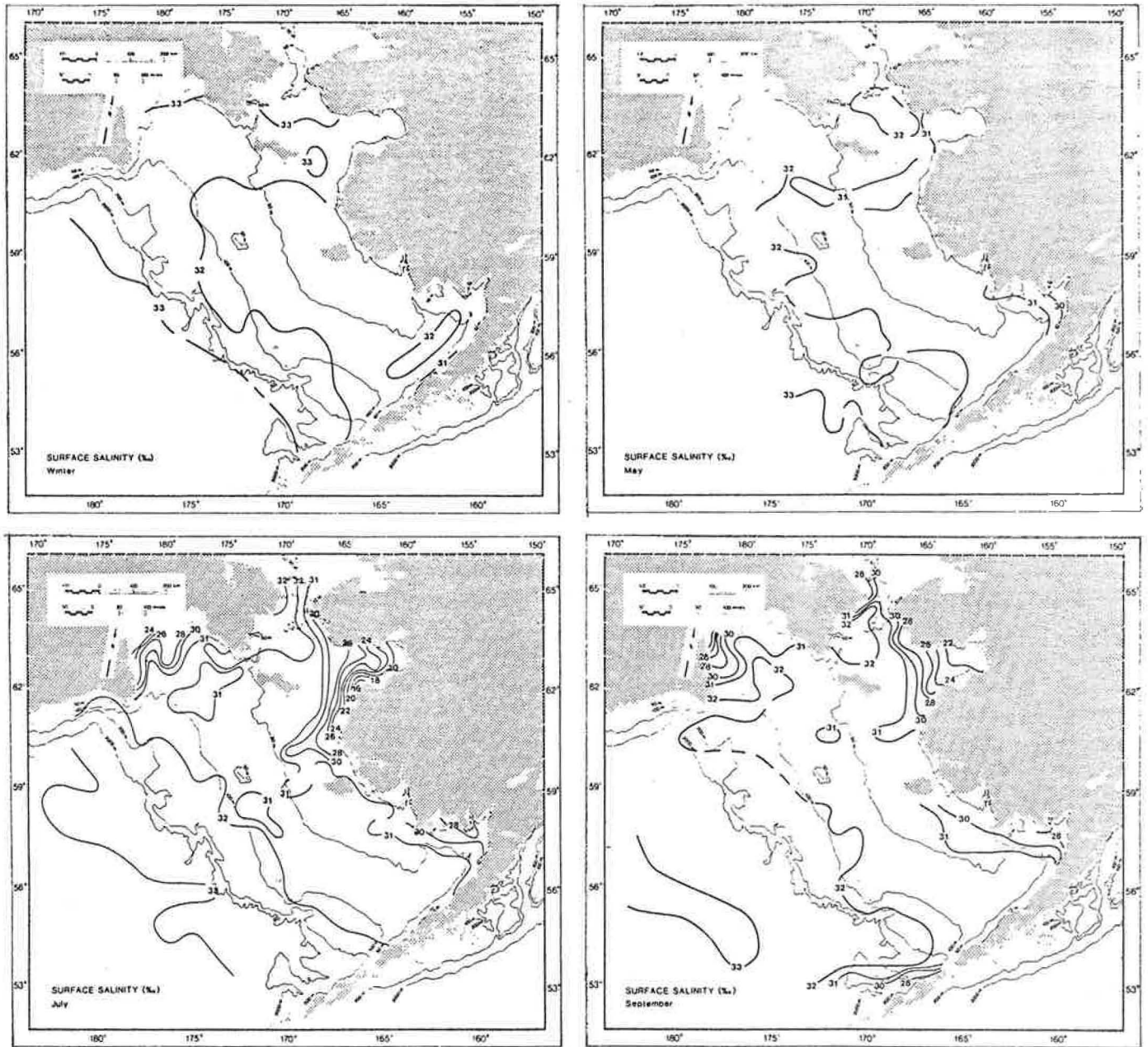


Figure 25.--Long-term mean sea surface salinity (‰) for January to March, May, July, and September (Ingraham, 1981).

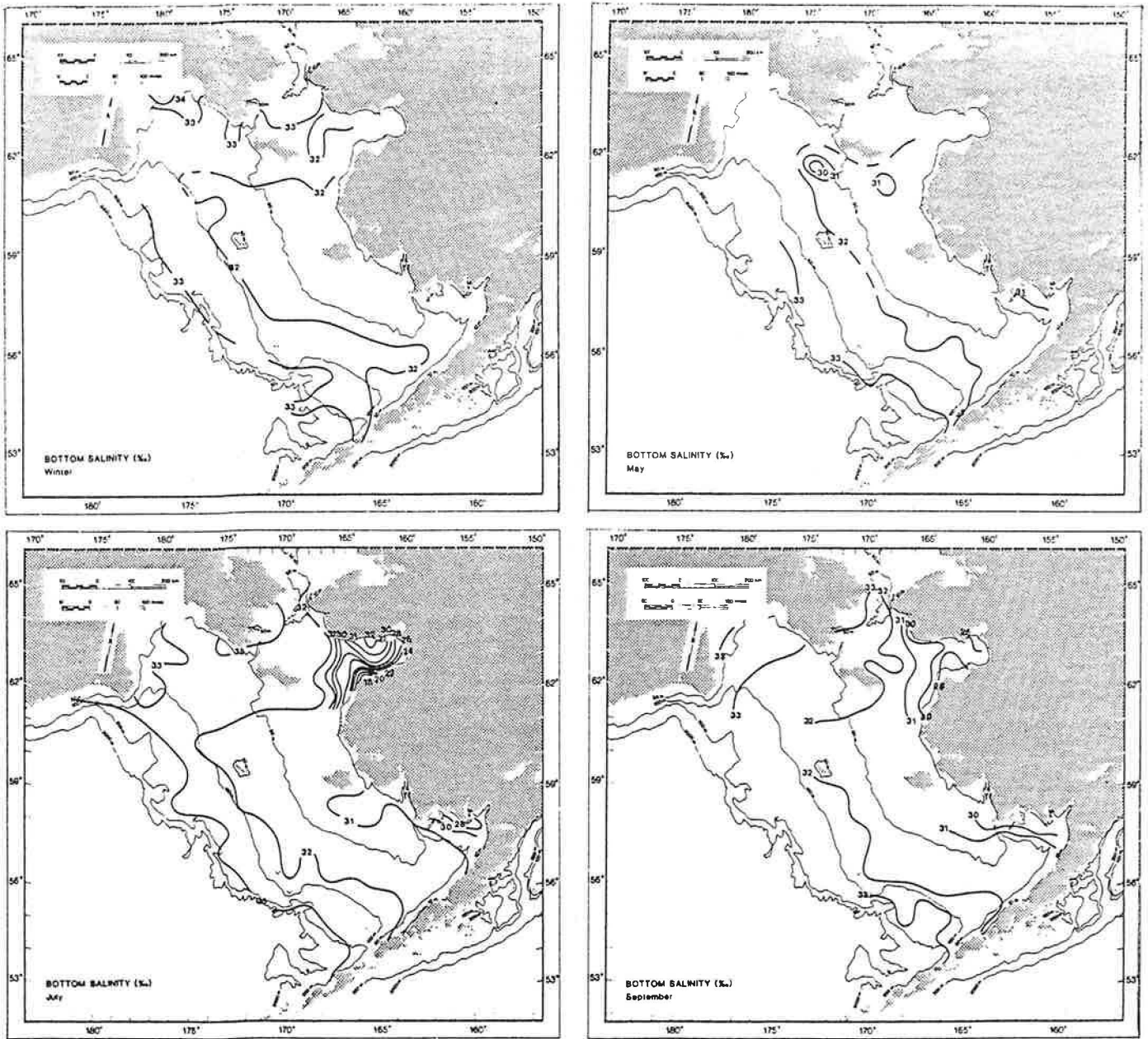


Figure 26.--Long-term mean bottom salinity (‰) for January to March, May, July, and September (Ingraham, 1981).

### Vertical water structure and seasonal changes

In a synthesis of recent hydrographic data from the southeastern Bering Sea, Kinder and Schumacher (1981) characterized the shelf as having three distinct temperature, salinity, and water structure domains separated by fronts which lie near the 50 and 100 m depth contours (Figure 27). Inshore, the coastal domain (0 to 50 m depth range) has no significant vertical structure, for it is well mixed by consistently strong tidal currents except in local areas which are under the direct influence of river discharge. The middle shelf domain (50 to 100 m depth range) varies from being well mixed during winter when surface cooling and more frequent and stronger storms assist tidal mixing, to being two-layered in summer when buoyancy additions from melting ice and solar insolation exceed tidal and wind mixing. The inner front is a narrow (about 10 km) transition zone at the balance between tidal mixing and buoyant energy input (Schumacher, et al., 1979). The outer domain (100 to 170 m depth range) is three-layered throughout the year, a well-mixed upper layer, a well-mixed higher temperature and higher salinity lower layer, and a stratified interior layer between about 40 and 70 m depth containing a considerable amount of finestructure from interleaving of water masses on vertical scales from 1 to 25 m (Coachman and Charnell, 1977, 1979). The middle front, between the middle and the outer domain, is broader (about 50 km) than the inner front (about 10 km) and it occurs coincidentally with the steepening (five fold) of the bathymetry around the 100 m depth contour. Present data do not show great changes in the location of these fronts on diurnal, fortnightly, or interannual time scales.

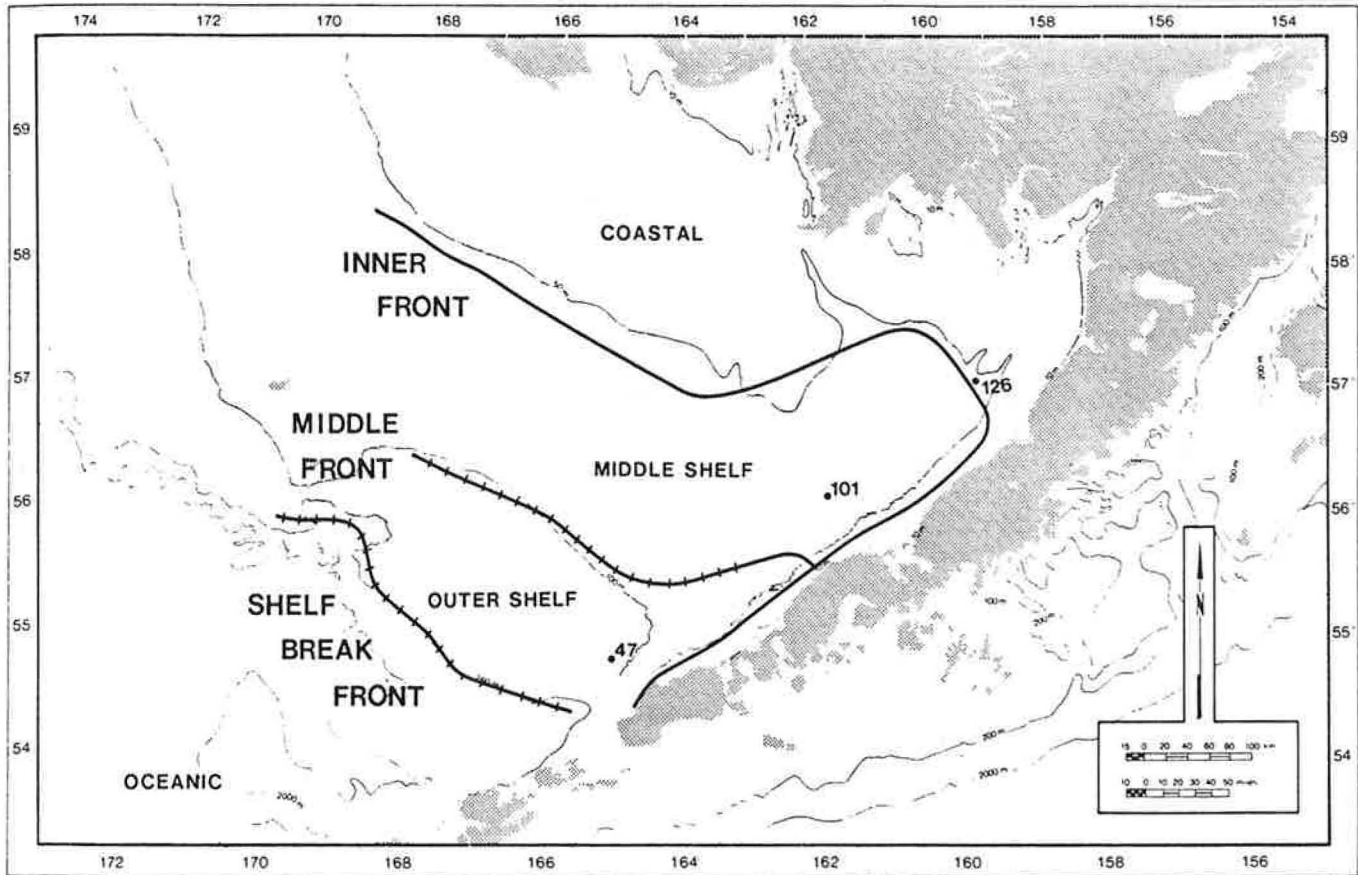


Figure 27.--Locations of the domains (coastal, middle, and oceanic) and fronts (inner, middle, and shelf break) over the eastern Bering Sea shelf (Kinder and Schumacher, 1981).

### Nutrient salts

The distributions and cycling of chemical nutrients (phosphate-P, nitrate-N, silicic acid-Si, nitrite-N, and ammonium-N) provide fundamental insight into the nature of biological productivity on the southeastern Bering Sea shelf which is supplied at depth by a nearly unlimited source of nutrients from the Bering Sea proper. In the annual cycle, the major feature is the sharp increase with depth which forms at the seasonal thermocline as nutrients are extracted from the euphotic layer (upper 10 to 50 m) by phytoplankton during spring and summer; this is followed by a gradual replenishment of nutrients during autumn and winter due to vertical mixing and biological-chemical regeneration. Hattori and Goering (1981) reviewed available data and showed that the horizontal features of the nutrient distributions conformed closely to the hydrographic domains (coastal, mid-shelf, outer-shelf, and oceanic) discussed earlier. By comparing temperature, phosphate, nitrate, and silicic acid versus salinity diagrams (Figure 28) they found the four distinct water masses illustrated as separate envelopes of data in the temperature versus salinity diagram and also four corresponding envelopes of data in each of the three nutrient-salinity diagrams. Because the data covered several years, they concluded that the zonation of nutrients is a general feature of the southeastern Bering Sea in summer. Thus, two general trends in the distribution of nutrient concentrations are apparent: (1) a gradual offshore increase which changes in steps at fronts between hydrographic domains, and (2) an increase with depth in one large step in the seasonal thermocline which exists seaward of the constantly well stirred coastal domain. A notable exception is in the ammonium distribution which drops off to a very low ( $<0.5$  g at N/1) concentration in the outer-

shelf and oceanic domains below 75 m, leaving a distinct mid-shelf maximum near bottom and a weaker maximum in the outer-shelf thermocline (30-50 m) (Figure 29). The nitrite distribution is similar to that of ammonium.

Ratios of concentrations between major nutrients indicate that the eastern Bering Sea is similar to other ocean areas in terms of global averages with atoms of nitrate-N/phosphate-P about 15:1 and atoms of silicic acid-Si/phosphate-P about 33:1, but deviations from these established ratios locally indicate significant variation in nutrient cycling which is apparently caused by a major separation in food webs at the middle front. The lowest ratios in nitrate-N/phosphate-P (about 5:1) are found in the mid-shelf bottom water, and intermediately lower ratios (about 10:1) occur in the outer-shelf euphotic layer. Both coincide with maxima in the vertical ammonium distributions, indicating areas where phosphate is regenerated faster than nitrate. The lowest ratio in silicic acid-Si/phosphate-P also occurs in the mid-shelf bottom water, again phosphate apparently regenerating more rapidly than silicic acid. In contrast, Si/P ratios higher than the norm do occur randomly over the entire area but only in the euphotic layer when diatoms which require silicic acid are low in numbers, then silicic acid is underutilized relative to phosphate. Reasons for these nutrient distributions, although not varified extensively by large field data sets, become clearer when the outer-shelf and inner-shelf food webs are considered.

Physical, hydrographic processes which restrict the advective exchange of water and its contents across the middle front appear to be the chief cause for the horizontal structuring of nutrient distributions and food

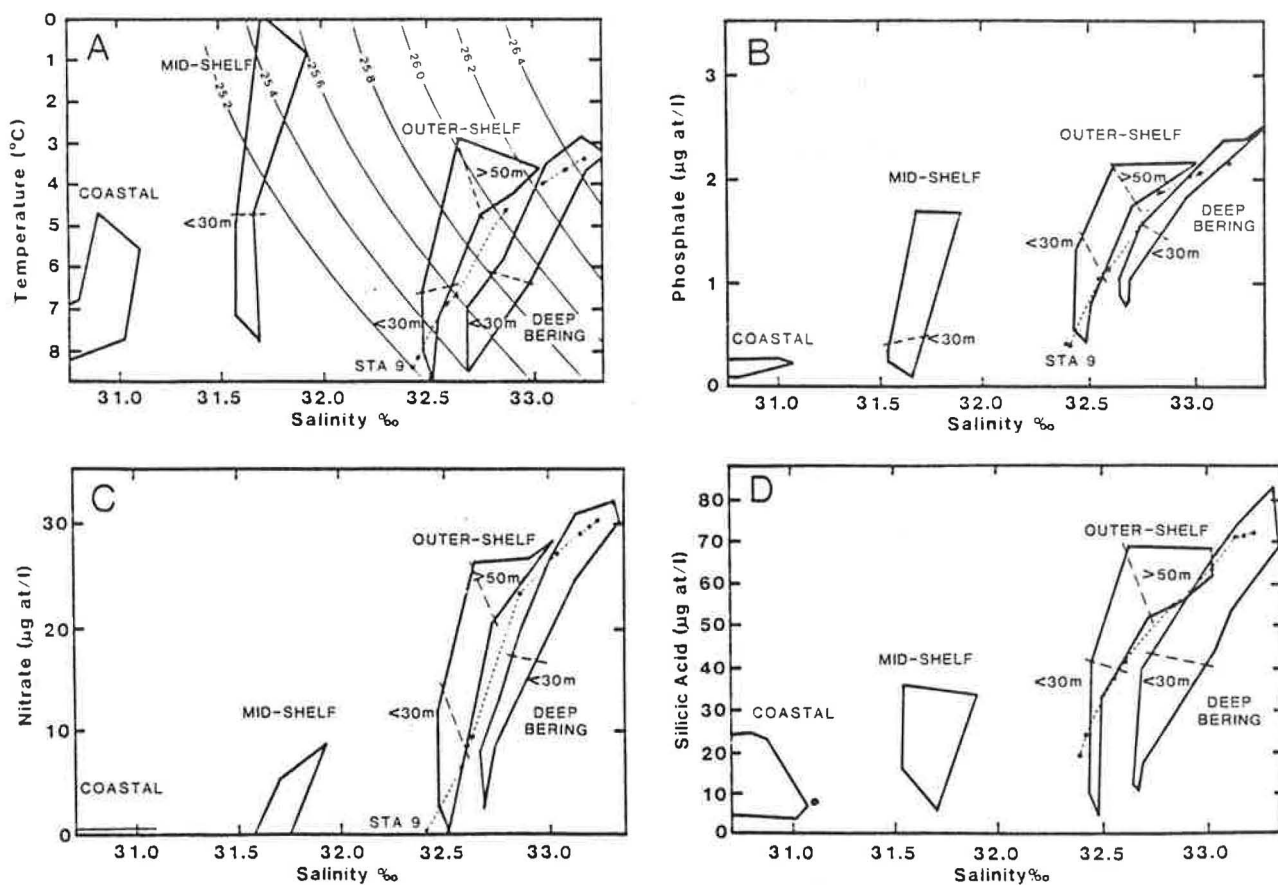


Figure 28.--Temperature-salinity and nutrient-salinity envelopes in the eastern Bering Sea in July 1978 (Hattori and Goering, 1981).

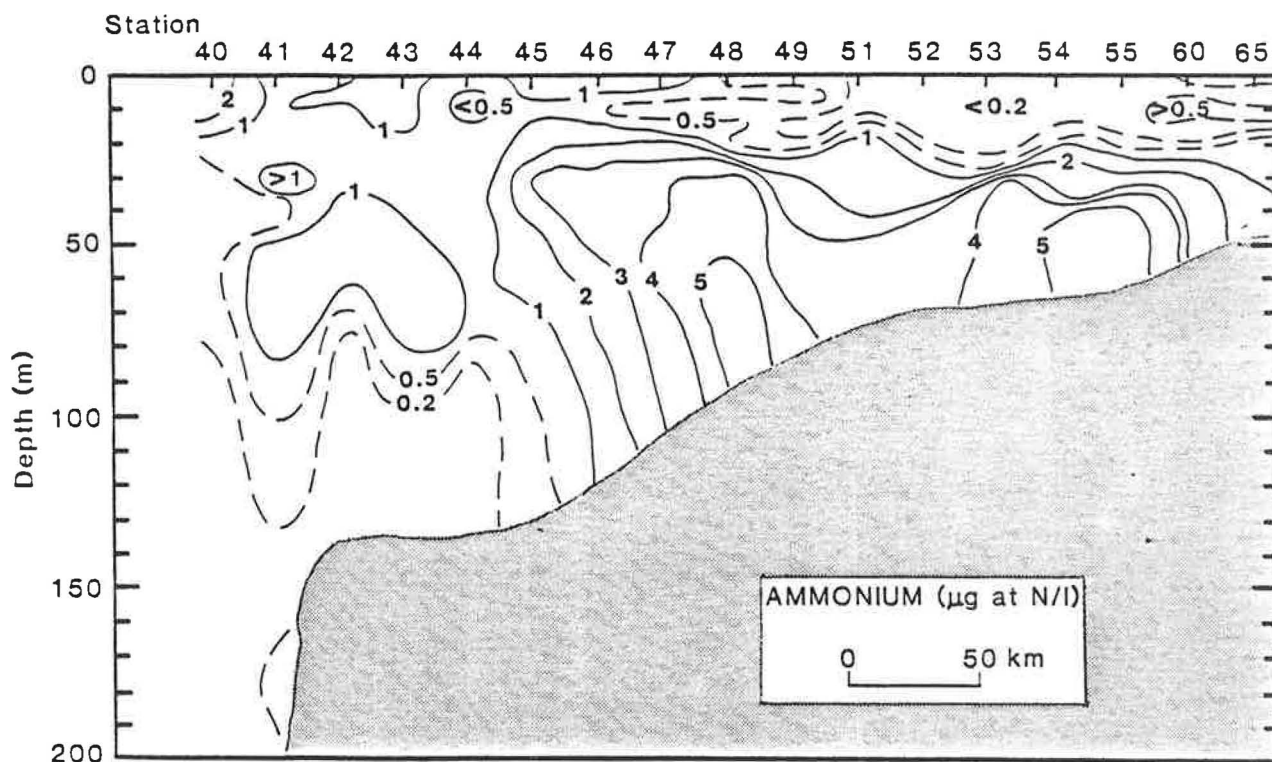


Figure 29.--Ammonium ( $\mu\text{g at N/l}$ ) cross section in outer Bristol Bay south of Pribolif Islands during 29-31 May 1979 (Hattori and Goering, 1981).

webs on this shelf. The phytoplankton consist mainly of diatoms and microflagellates. The flagellates being more numerous during winter, give way to a major diatom bloom in April which sets the diatom dominance for the rest of the summer. The herbivores which graze on these phytoplankton during spring and summer are segregated by the minimal exchange at the middle front. On the outer-shelf the large standing stock of large sized calanoid copepods and euphausiids effectively graze even the large summer diatoms. The results are: 1) a small standing stock of phytoplankton flagellates and dinoflagellates, 2) an extended supply of nutrients to the euphotic layer by regeneration, and 3) a subsurface maximum concentration of ammonium most likely from the excretion of zooplankton. Thus, the outer-shelf has a pelagic food web. In the mid-shelf domain contrasting conditions occur because the zooplankton are small and unable to effectively graze the large diatoms. This results in: 1) a small standing stock of zooplankton, 2) a flourishing large standing stock of large diatoms with large nutrient demands, 3) a continuous rain of unconsumed diatoms to the sea bed, and 4) a benthic nutrient regeneration cycle with large concentrations of near-bottom chlorophyll-a and ammonium. Thus, the mid-shelf has a benthic food web.

### Dissolved hydrocarbons

The distributions of dissolved low molecular weight hydrocarbons in Bristol Bay were summarized by Cline (1981) who described their usefulness as a diagnostic indicator of petroleum hydrocarbons. Although the alkanes (methane, ethane, propane and butane) which are abundant constituents of crude oil and natural gas were present in Bristol Bay waters, their low concentrations, relatively high methane/ethane plus propane ratio of 30 to 500, and low ethane/ethene ratio of less than 1.0 all suggest a biological source. Cline, therefore, concluded that Bristol Bay is "pristine" and discussed his base line data on the naturally occurring biogenic hydrocarbons.

Methane is the dominant low molecular weight hydrocarbon appearing in concentrations of about two orders of magnitude greater than ethane, ethene, propane, and propene (Table 3). Despite the July maximum compared to September-October data, the major features of the methane distribution generally conform to the hydrographic domains with highest concentrations occurring (from lagoons) in the coastal domain, low concentrations near saturation in the mid-shelf domain, and intermediate values in the outer-shelf domain (Figure 30a). Higher values up to 12 fold of saturation near bottom in the outer-shelf domain (Figure 30b) suggest an additional source in the organic-rich sediments of the outer-shelf.

In contrast to methane, concentrations of the higher carbon number hydrocarbons (ethane, ethene, propane, and propene) were governed more by seasonal biological processes than frontal dynamics. For example, the surface distribution of ethene in summer (Figure 31) shows highest values in eastern Bristol Bay, then values gradually decrease westward with no well defined source and little, if any, influence by the 50 m front. Higher values at

Table 3.--Average (a) surface and (b) near-bottom concentrations (nl/l, STP) of methane, ethane, ethene, propane, and propene for various water depth intervals (Cline, 1981).

CRUISE	DOMAIN		METHANE		ETHANE		ETHENE <sup>1</sup>		PROPANE		PROPENE <sup>1</sup>	
			Mean	Range	Mean	Range	Mean	Range	Mean	Range	Mean	Range
Sept.-Oct., 1975	Coastal (<50 m)	a	64	45-94	--	--	0.9	0.3-1.7	--	--	0.5	0.2-1.1
		b	59	45-98	--	--	1.0	0.7-1.8	--	--	0.4	0.1-0.6
	Middle Shelf (50-100 m)	a	60	42-83	--	--	0.8	0.3-1.6	--	--	0.4	0.1-1.1
		b	99	65-163	--	--	1.7	1.2-2.7	--	--	0.6	0.3-1.3
	Outer Shelf (100-200 m)	a	76	40-200	--	--	0.5	0.2-0.8	--	--	0.3	0.3-0.4
		b	380	100-615	--	--	1.1	0.7-1.6	--	--	0.3	0.2-0.4
June-July, 1976	Coastal (<50 m)	a	112	74-153	0.9	0.6-1.5	3.8	3.0-4.7	0.4	0.3-0.6	1.4	1.0-2.5
		b	114	73-153	1.0	0.5-2.5	3.4	2.3-4.4	0.4	0.2-0.6	1.2	0.7-1.6
	Middle Shelf (50-100 m)	a	85	52-134	0.6	0.3-1.5	2.9	1.9-4.7	0.3	0.2-0.6	1.1	0.6-1.7
		b	115	62-165	1.3	0.5-2.5	2.2	1.1-4.0	0.5	0.3-0.6	0.5	0.2-1.0
	Outer Shelf (100-200 m)	a	140	53-276	1.1	0.4-2.1	2.3	1.8-2.8	0.4	0.2-0.7	0.7	0.5-1.1
		b	269	164-440	0.9	0.6-1.1	1.2	0.8-1.8	0.3	0.2-0.4	0.3	0.1-0.9

<sup>1</sup>Due to analytical difficulties encountered during the Sept.-Oct. 1975 cruise, concentrations of ethene and propene include ethane and propane respectively.

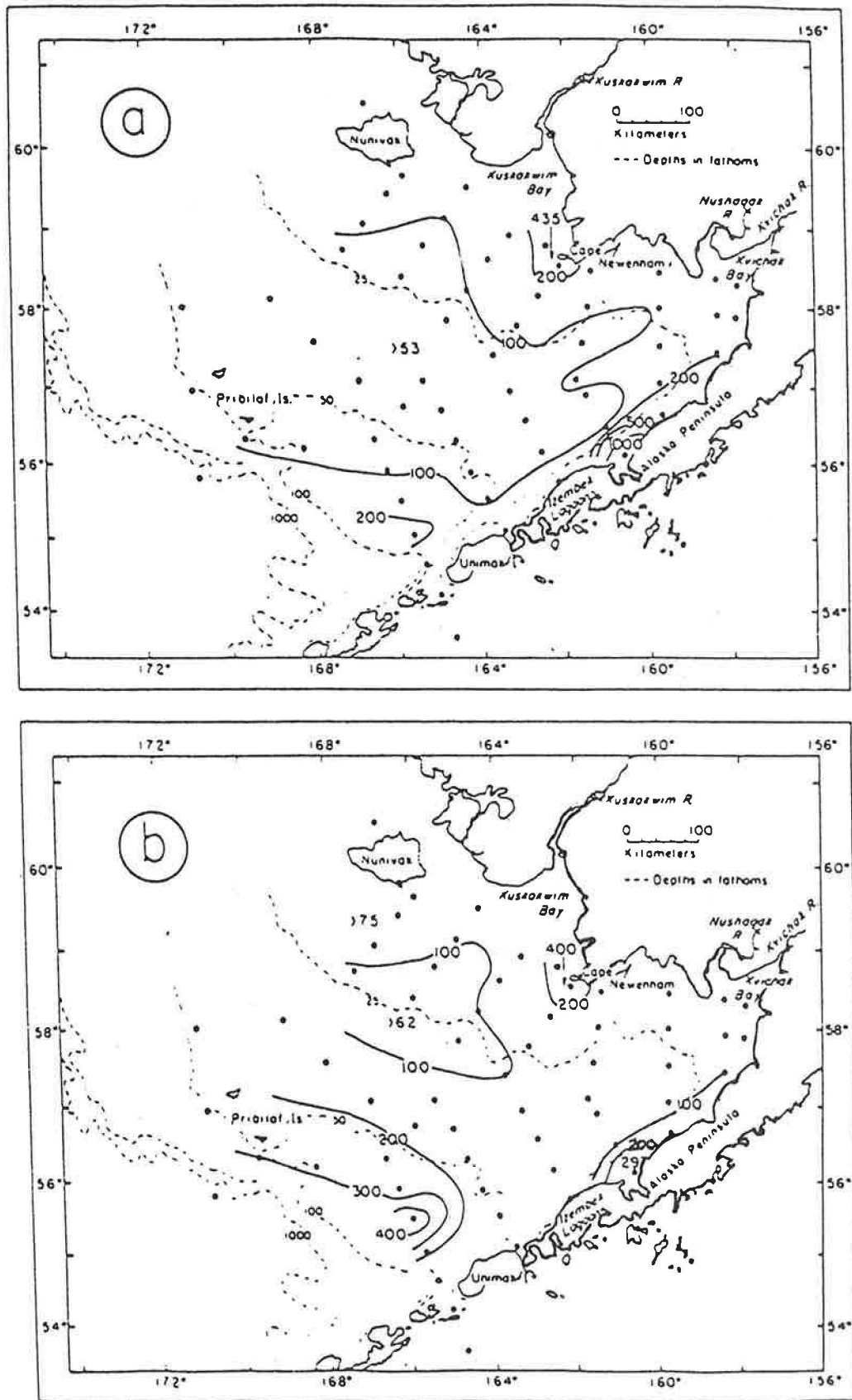


Figure 30.--(a) Surface and (b) near-bottom distributions of dissolved methane during July 1976 (Cline, 1981).

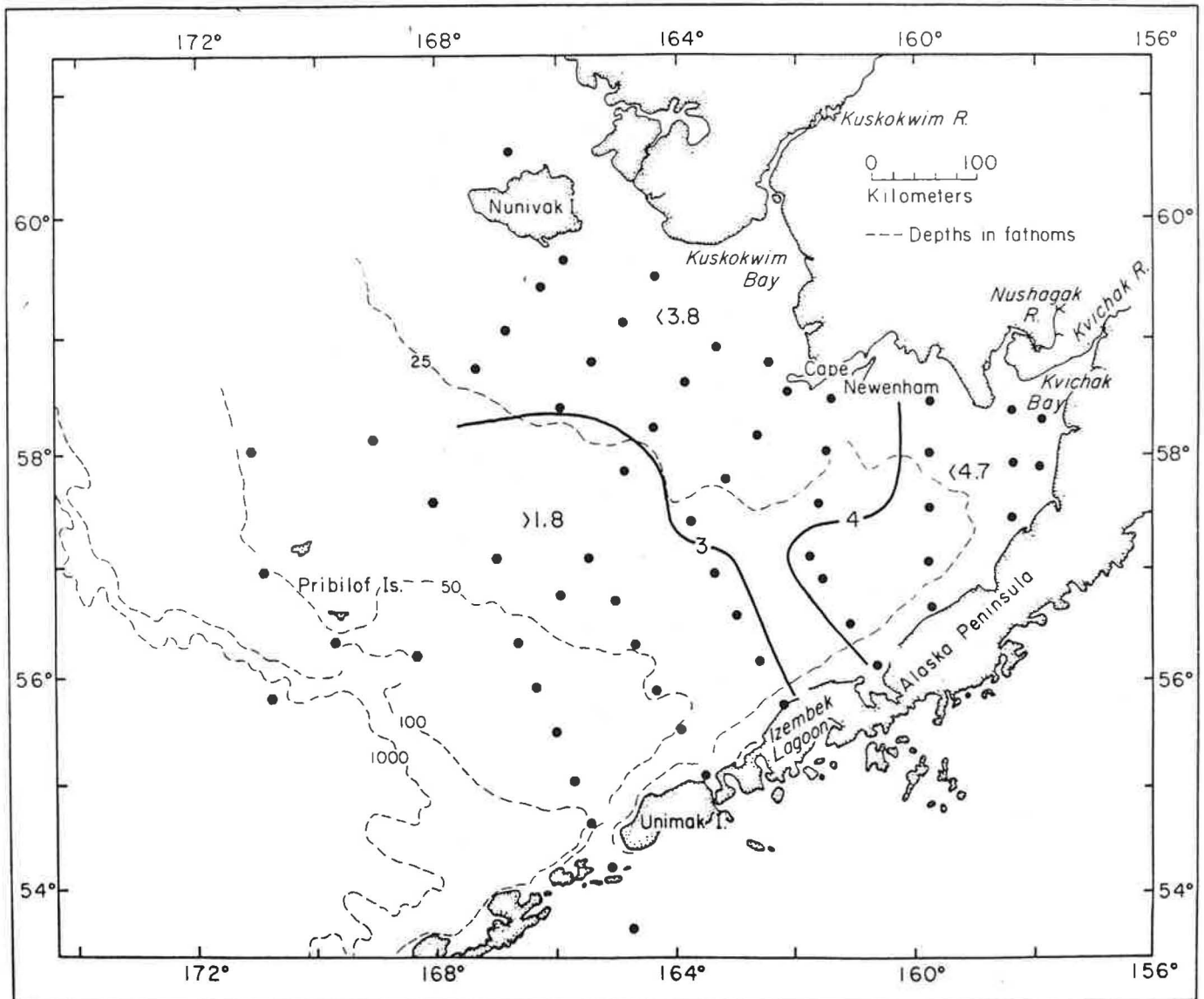


Figure 31.--Surface distribution of dissolved ethene (nl/l, STP) in July 1976 (Cline, 1981).

depth in the fall, higher values at the surface in summer, and the nearly doubling of all values in summer may be attributed to seasonally increased biological or induced photo-chemical production in the surface layers. Ethene is consistently related to ethane at a 3 to 1 ratio. Similar trends are shown in the propene and propane distributions and ratios; but because of their lower concentrations, seasonal and spatial variations are more obscure. Butane concentrations were always below the detection threshold of 0.05 nl/l.

- Arsen'ev, V.S. 1967. The currents and water masses of the Bering Sea.  
(Trans. 1968. Natl. Mar. Fish. Serv., Northwest & Alaska Fisheries  
Center, Seattle, WA), 146 pp.
- Bacon, J.C. 1973. Numerical investigation of Bering Sea Dynamics. M.S.  
Thesis. U.S. Naval Postgraduate School, Monterey, CA., 62 p.
- Baker, E.T. 1983. Suspended particulate matter distribution, transport,  
and physical characteristics in the north Aleutian Shelf and St. George  
Basin lease areas. OCSEAP Report: RU 594, 134 pp.
- Barns, C.A., and T.G. Thompson. 1938. Physical and chemical investigations  
in Bering Sea and portions of the North Pacific Ocean. Univ. of  
Washington Press, Seattle, WA, 161 p.
- Bezrukov, P.L. (ed.). 1959. Geographical description of the Bering Sea:  
Bottom relief and sediments. Trans. by Israel Program for Scientific  
Translations, Jerusalem, U.S. Dep. of Commer., Natl. Sci. Foundation,  
Washington, D.C., 188 p.
- Brower, W.A., H.F. Diaz, A.S. Prectel, H.W. Searby, and J.L. Wise. 1977.  
Climactic atlas of the outer Continental Shelf waters and coastal regions  
of Alaska. Vol. II: Bering Sea. AEIDC and NOAA, OCSEAP, RU347, Anchorage  
AK, 443 p.
- Cline, J.D. 1981.  
Distributions of Dissolved LMW Hydrocarbons in Bristol Bay, Alaska:  
Implications for Future Gas and Oil Development. In: The Eastern  
Bering Sea Shelf; oceanography and resources, Vol. 1, D.W. Hood  
and J.A. Calder, eds. NOAA, Office of Marine Pollution Assessment,  
pp 425-444.
- Coachman, L.K., and R.L. Charnell. 1977. Fine structure in outer Bristol Bay,  
Alaska. Deep-Sea Research 24, pp 869-889.

- Coachman, L.K., and R.L. Charnell. 1979. On lateral water mass interaction -- A case study, Bristol Bay, AK. *J. of Phys. Ocean*, Vol. 9, #2, pp. 278-297.
- Demory, R.L., R.F. Orrell, and D.R. Heinle. 1964. Spawning ground catalog of the Kvichak River system, Bristol Bay, AL. U.S. Dep. of Interior, Fish & Wildlife Service, Spceial Scientific Report, Fisheries #488, 292 p.
- Dodimead, A.J., F. Favorite, and T. Hirano. 1963. Salmon of the North Pacific Ocean - Part II. Review of oceanography of the Subarctic Pacific region. *Int. North Pac. Fish. Comm. Bull.* 13, 195 p.
- Durrenberger, R.W. 1980. Alaska solar and weather information, one in a series of thirteen climate data manuals for the states of the western region. Western Sun Pub., Portland, OR, pp 1-67.
- Favorite, F. 1974. Flow into the Bering Sea through Aleutian Island passes. In: *Oceanography of the Bering Sea; with emphasis on renewable resources*, D.W. Hood and E.J. Kelley, eds. *Inst. Mar. Sci., Univ. of Alaska, Occ. Pub. No. 2*, pp 3-39.
- Favorite, F., A.J. Dodimead, and K. Nasu. 1976. Oceanography of the Subarctic Pacific Region, 1960-1971. *Int. North Pac. Fish. Comm. Bull. No. 33*.
- Feely, R.A., G.J. Massoth, A.J. Paulson, M.F. Lamb, and E.A. Martin. 1981. Distribution and elemental composition of suspended matter in Alaskan coastal waters. *NOAA Tech. Memo. ERL PMEL-27*, 119 p.
- Hattori, A., and J.J. Goering. 1981. Nutrient distributions and dynamics in the Eastern Bering Sea. In: *The Eastern Bering Sea Shelf; oceanography and resources*, Vol. 2, D.W. Hood and J.A. Calder, eds. *NOAA, Office of Marine Pollution Assessment*, pp. 975-992.
- Hebard, J.F. 1961. Currents in Southeastern Bering Sea. *Bull. Int. North Pac. Fish. Comm. No. 5*, pp 9-16.

- Marriott, R.A., N. Aspihwall, T.S.Y Koo, and R.L. Burgner. 1964. Stream catalog of the Wood River lake system, Bristol Bay, AK. U.S. Dep. of Int., Fish and Wildlife Service Special Scientific Report No. 494, 210 pp.
- McDonald, J., H.M. Feder, and M. Hoberg. 1981. Bivalve mollusks of the Southeastern Bering. In: The Eastern Bering Sea Shelf: oceanography and resources, Vol. 2. D.W. Hood and J.A. Calder, eds. NOAA, Office of Marine Pollution Assessment, pp 115-1204.
- McLain, D. R., and F. Favorite. 1976. Anomalously cold winters in the Southeastern Bering Sea, 71-75. Marine Sciences Communications 2(5), pp. 299-334.
- McRoy, C. P., J. J. Goering, and W. E. Shiels. 1972. Studies of primary production in the Eastern Bering Sea. In: Biological Oceanography in the Northern North Pacific Ocean, A. Y. Takenouti, chief ed. Indentisu Shoten, Tokyo. pp. 199-216.
- Nakajima, Kohhi. 1969. Suspended particulate matter in the waters on both sides of the Aleutian Ridge. Journal Oceanogr. Soc. Japan Vol. 25, No. 5, pp. 239-248.
- Pearson, C. A. 1981. Guide to R2D2 - Rapid retrieval data display. NOAA Tech. Memo. ERL PMEL-29.
- Pearson, C. A., H. O. Modjeld, and R. B. Tripp. 1981. Tides of the Eastern Bering Sea Shelf. In: The Eastern Bering Sea Shelf: oceanography and resources, Vol. 1, D. W. Hood and J. A. Calder, eds., NOAA Office of Marine Pollution Assessment, pp. 110-130.
- Pola Swan, N., and W. J. Ingraham, Jr. 1984. Numerical Simulation of the Effect of Interannual Temperature Fluctuations on Fish Distribution in the Eastern Bering Sea. NOAA Tech. Memo., NMFS F/NWC 57-60 pp.
- Reed, R. K. 1977. On estimating insulations over the ocean. J. of Phys. Oceanography No. 7, pp. 482-485.

- Reed, R. K. 1978. The heat budget of a region in the Eastern Bering Sea, summer 1976. *J. of Geophys. Res.*, Vol. 83, No. C7, pp. 3635-3645.
- Roden, G. I. 1967. On river discharge into the Northeastern Pacific Ocean and the Bering Sea. *J. of Geophys. Res.* Vol. 72, No. 22, pp. 5613-5629.
- Ruffner, J. A. 1978. *Climates of the states, with current tables of normals 1941-1970 and means and extremes to 1975*, Gale Research Company Press.
- Schumacher, J. D., T. H. Kinder, D. J. Pashinski, and R. L. Charnell. 1979. A structural front of the continental shelf of the Eastern Bering Sea. *J. of Phy Ocean*; Vol. 9, No. 1, pp. 79-87.
- Sharma, G. D. 1979. *The Alaskan Shelf, hydrographic, sedimentary, and geochemical environment*. Springer-Verlag, New York, pp. 272-369.
- Straty, R. R. 1977. Current patterns and distributions of river waters in Inner Bristol Bay, AK. NOAA Tech. Rep., NMFS SSRF-713, 13 pp.
- Stringer, W. J. 1981. Nearshore ice characteristics in the Eastern Bering Sea. In: *The Eastern Bering Sea Shelf: oceanography and resources*, Vol. 1, D. W. Hood and J. A. Calder, eds. NOAA, Office of Marine Pollution Assessment, pp. 167-188.
- Sugiura, Y. 1974. Phosphate and oxygen problems with reference to water circulations in the Subarctic Pacific Region. In: *Oceanography of the Bering Sea, with emphasis on renewable resources*, D. W. Hood and E. J. Kelley, eds. *Inst. of Mar. Sci., Univ. of Alaska*, Oco. Pub. No. 2, pp. 163-172.
- Tanoue., and N. Handa. 1979. Distribution of particulate organic carbon and nitrogen in the Bering Sea and northern North Pacific Ocean. *Journal of Ocean. Soc. of Japan*, Vol. 35, No. 1., pp. 47-62.